	Ni
16	Cr
8.5	Co
3.5	Al
3.5	Ti
2.6	W
1.8	Mo
0.9	Cb

IN-738

1 GENERAL

IN-738 is a heat-treatable nickel-base casting alloy with mechanical properties comparable to those of Inconel 713C but with substantially better resistance to hot corrosion (also called sulfidation). Consequently, it provides good creep strength at temperatures up to 1800 F combined with good resistance to the hot corrosive environments associated with gas turbines. The high strength of IN-738 is a result of the following mechanisms: solid-solution strengthening from chromium, molybdenum, tungsten, and cobalt; precipitation hardening from a gamma-prime phase consisting of nickel-aluminum-titanium compounds; and grain boundary strengthening from carbides and borides. Its superior hot corrosion resistance over Inconel 713C is affected by increased chromium, cobalt, tantalum, and titanium contents and decreased molybdenum content. On the other hand, the lower aluminum content of IN-738 results in decreased oxidation resistance. A slightly modified version of the alloy, designated IN-738LC, has lower carbon and zirconium contents for improved castability, particularly in large section sizes. The modification has only minor effects on mechanical properties and corrosion resistance. IN-738 is used primarily for jet engine and gas turbine components, such as blades, vanes, and integral wheels, requiring good resistance to hot corrosion (1-6,12,21).

1.01 Commercial Designation

IN-738 and low-carbon version, IN-738LC.

1.02 Alternate Designations

Alloy IN-738, IN-738C, and Nimonocast IN-738.

1.03 Specifications

No AMS, ASTM, military, or federal specifications covering IN-738 have been published.

1.04 Composition

Composition, Table 1.04.

1.05 Heat Treatment

1.051 The alloy is normally used in the precipitation-hardened condition, which provides its optimum combination of mechanical properties. The following solution and precipitation cycle is most commonly applied: solution treat 2 hr at 2050 F, air cool to room temperature, precipitation harden 24 hr at 1550 F, air cool. In some instances a shorter precipitation-hardening time of 16 hr has been used (2,12,19).

1.06 Hardness

1.061 Effects of aging for 16 hr at various elevated temperatures on hardness of solution-treated material at room temperature, Figure 1.061.

1.062 Effects of long-term exposures to temperatures from 1380 to 1560 F on hardness at room temperature, Figure 1.062.

1.07 Forms and Conditions Available

IN-738 is available principally in the form of investment castings. These castings can be supplied either in the as-cast or precipitation-hardened condition (2).

1.08 Melting and Casting Practices

IN-738 is normally vacuum melted and vacuum-investment cast with procedures similar to those used for other cast nickel-base superalloys. Typical casting conditions are: 200 to 400 F superheat above the liquidus temperature and mold preheat 1500 to 1800 F. These conditions vary somewhat depending upon the size and configuration of the parts (2).

1.09 Special Considerations

1.091 Like other cast alloys, particularly in the larger section sizes, IN-738 is subject to the formation of microporosity during solidification, which detracts from mechanical properties. Good foundry practice can minimize but not always prevent this problem. Hot isostatic pressing (HIP), which involves externally pressurizing the castings in argon at a high temperature, can be used to at least partially eliminate microporosity and its detrimental effects on IN-738. (See Tables 3.0212, 3.0317, 3.0418, and Figure 3.057.)

1.092 The properties of IN-738, like castings in general, are usually isotropic. Anisotropy, however, can be achieved with directional solidification, which results in superior properties, usually but not invariably, in the longitudinal direction (parallel to the solidification direction). (See Figures 3.0416, 3.0512, and 3.0513.)

1.093 Long-term exposures to elevated temperatures near or above the aging temperature cause reduced strength and ductility in IN-738. (See Figure 3.0231, 3.0316, 3.049, 3.0412, 3.0413, 3.0414, and 3.0510.) At least a portion of the deterioration is a result of overaging, that is, the agglomeration of the nickel-aluminum-titanium precipitation-hardening phase, gamma prime. When the elevated-temperature exposures are carried out in air, however, a greater amount of the deterioration is caused by oxygen damage, to which all nickel-base superalloys are sensitive (37). (See Figures 3.0410 and 3.054.) Oxygen damage can be inhibited by a suitable protective coatings. (See Figure 3.0411 and Section 4.042.) Recent research indicates that small additions of hafnium and increases in boron content substantially decrease susceptibility to oxygen damage in IN-738 (37).

2 PHYSICAL AND CHEMICAL PROPERTIES

2.01 Thermal Properties

2.011 Melting range, 2250 to 2400 F (2).

2.012 Phase changes.

2.0121 Time-temperature-transformation diagrams.

2.0122 In the solution-treated condition, IN-738 consisted of a nickel-base solid solution with a small amount of carbides and gamma prime,

Ni
16 Cr
8.5 Co
3.5 Al
3.5 Ti
2.6 W
1.8 Mo
0.9 Cb

IN-738

which is a compound of nickel, aluminum, and titanium, in the microstructure. Aging at temperatures above 1000 F causes precipitation of additional finely dispersed gamma prime, which increases strength and hardness; overaging at excessive temperatures or for excessive times, however, causes agglomeration of the gamma prime with associated decreases in hardness and strength. (See Figure 1.061.) The optimum degree of precipitation of gamma prime and optimum mechanical properties are achieved by the standard aging treatment of 1550 F for 24 hr. Higher aging temperatures or excessive times at lower temperatures cause overaging. Aging at temperatures above about 1900 F causes gradual resolution of the gamma-prime elements, aluminum and titanium, which results in room-temperature hardness and strength exceeding those of the overaged material. All of the gamma prime is taken into solid solution at 2135 F (solvus temperature) and above. Carbides remain almost unchanged with elevated temperature exposures up to 2050 F. Some solutioning of carbides occurs above 2050 F but complete solutioning never occurs up to 2200 F. The fact that the normal solution-treating temperature of 2050 F is below the solvus temperatures for both gamma prime and carbides accounts for the presence of small amounts of these constituents in the solution-treated material (12).

2.0123 IN-738 has good resistance to the formation of sigma and other brittle phases, which can be detrimental to both toughness and corrosion resistance. No such phases have formed in IN-738 exposed for 6000 hr to 40 ksi tensile stress at 1500 F, which is normally within the most sensitive temperature range for sigma formation. To ensure optimum resistance to the formation of brittle phases, the composition of the alloy should be balanced to achieve an electron-vacancy number (Nv) below 2.36. A method for calculating Nv is given in Reference 2 (2,22,24).

2.013 Thermal conductivity, Figure 2.013.

2.014 Thermal expansion, Figure 2.014.

2.015 Specific heat, Figure 2.015.

2.016 Thermal diffusivity.

2.02 Other Physical Properties

2.021 Density, 0.293 lb/in.^{3} and 8.11 gr/cm^3 (2).

2.022 Electrical properties.

2.023 Magnetic properties.

2.024 Emittance.

2.025 Damping capacity.

2.03 Chemical Properties

2.031 Numerous tests carried out by various investigators have shown the oxidation resistance of IN-738 to be somewhat inferior to that of Inconel 713C. However, its resistance to hot corrosion (sulfidation) is far superior to 713C, particularly in environments containing sodium sulfate and sodium chloride similar to those to which blades and other hot components of gas turbines are exposed in service.

2.0311 Comparison of the resistance of IN-738 and 713C to oxidation and to hot corrosion, Table 2.0311.

2.0312 In oxidation tests in still air for 100 hr, during which samples were continuously cycled 1 hr at 2010 F and then cooled for 40 minutes, the weight loss was 28 mg/cm^2 for IN-738, but less than 5 mg/cm^2 for 713C and two other nickel-base superalloys – VIA and B-1900. The latter three are higher in aluminum content and lower in chromium content than IN-738. On the other hand, when the same alloys were coated with sodium sulfate prior to oxidation, the primary attack changed to hot corrosion and the relative rates of attack reversed. IN-738 showed much greater resistance to attack than the other three alloys (27).

2.032 Oxidation.

2.0321 When exposed to still air at 1800 F and 2100 F for 1000 hr, IN-738 lost 16 and 102 mg/cm^2, respectively, due to the formation of loose oxide scale that did not adhere; whereas, 713C gained 0.6 and 29 mg/cm^2, respectively, due to the formation of an adhering oxide scale. In similar 1000-hr tests at 1800 F, except the samples were cycled to room temperature once each day, the IN-738 samples lost 14 mg/cm^2; but 713C lost only 0.7 mg/cm^2 (2).

2.033 Hot corrosion (sulfidation).

2.0331 The hot-corrosion resistance of IN-738 has been compared with that of a number of other nickel-base superalloys in several evaluation tests. Many of the tests involve exposures at elevated temperatures to a mixture of sodium sulfate and sodium chloride either in the form of a molten pool or in the form of a continuous or intermittent shower of particles (salt shower). Other tests involve exposures to the combustion gases of various types of fuels, sometimes with the addition of small amounts of sodium chloride to simulate sea conditions. Generally, these tests have shown the superiority of hot-corrosion resistance of IN-738 over 713C (two to a hundred times) depending upon the specific conditions. In one set of tests involving cyclic exposures to the exhaust gases from a gas turbine at 1780 F, IN-738 resisted hot corrosion six times better than 713C, three to five times better than MAR-M-246, VIA, and GMR 235D, and slightly better than Udimet 710. IN-939, however, which has higher chromium and cobalt contents, and MAR-M-509, which is a cobalt-base alloy, resist hot corrosion somewhat better than IN-738 (2,15).

2.0332 Effects of exposure time on weight loss due to hot corrosion of IN-738LC and four other nickel-base superalloys caused by exposures to a continuous salt shower of 75 percent sodium sulfate and 25 percent sodium chloride at 1560 F, Figure 2.0332.

2.0333 Effect of exposure temperature on time to formation of visible hot-corrosion products in environments of sodium sulfate and of sodium sulfate plus 10 percent sodium chloride, Figure 2.0333.

2.0334 Effects of time and temperature on depth of penetration of hot corrosion at atmospheric pressure in combustion gases from high-sulfur coal treated with dolomite as a sulfur suppressant, Figure 2.0334.

2.04 Nuclear Properties

3	MECHANICAL PROPERTIES
3.01	Specified Mechanical Properties
3.02	Mechanical Properties at Room Temperature
3.021	Tension – stress-strain diagrams – tension properties.
3.0211	Comparison of room-temperature tensile properties of regular and low-carbon grades of IN-738 produced in the form of cast-to-size specimens, Table 3.0211.
3.0212	Effects of hot isostatic pressing (HIP) on tensile properties at room temperature of specimens cast to size and machined from cast slabs, Table 3.0212.
3.0213	Tensile properties after vacuum melting and then casting in one and ten atmospheres of argon into two types of molds providing slow and fast freezing, Table 3.0213.
3.022	Compression – stress-strain diagrams – compression properties.
3.023	Impact.
3.0231	Effects of exposures to elevated temperatures in air on unnotched Charpy impact strength of fine-grain and coarse-grain castings, Figure 3.0231.
3.024	Bending.
3.025	Torsion and shear.
3.026	Bearing.
3.027	Stress concentration.
3.0271	Notch properties.
3.0272	Fracture toughness.
3.028	Combined properties.
3.03	Mechanical Properties at Various Temperatures
3.031	Tension – stress-strain diagrams – tension properties.
3.0311	Tensile properties of cast-to-size and heat-treated test bars in the temperature range 75 to 1800 F, Figure 3.0311.
3.0312	Tensile properties of cast-to-size and heat-treated test specimens at temperatures from 2000 to 2150 F, Figure 3.0312.
3.0313	Effects of temperatures up to 1500 F on tensile properties of cast-to-size specimens and machined specimens, Figure 3.0313.
3.0314	Tensile properties of as-cast, cast-to-size test bars in the temperature range 75 to 1800 F, Figure 3.0314.
3.0315	Tensile properties of the low-carbon version, IN-738LC, in the form of cast-to-shape and heat-treated test bars at temperatures up to 1650 F, Figure 3.0315.
3.0316	Effects of long-time exposures in air at 1560 and 1740 F on tensile and yield strengths of specimens tested at room temperature and 1600 F, Figure 3.0316.
3.0317	Effects of hot isostatic pressing (HIP) on tensile properties of the low-carbon version, IN-738LC, at room temperature and 1200 F. Test specimens machined from cast turbine blades, Table 3.0317.
3.032	Compression – stress-strain diagrams – compression properties.
3.033	Impact.
3.034	Bending.
3.035	Torsion and shear.
3.036	Bearing.
3.037	Stress concentrations.
3.0371	Notch properties.
3.0372	Fracture toughness.
3.038	Combined properties.
3.04	Creep and Creep-Rupture Properties
3.041	Creep-deformation and rupture curves at temperatures from 1300 to 1900 F, Figure 3.041.
3.042	Creep-deformation and rupture curves at 1300, 1500, and 1700 F, Figure 3.042.
3.043	Creep-rupture curves at temperatures from 1350 to 1800 F, Figure 3.043.
3.044	Creep-rupture curves at temperatures from 1290 to 1650 F for the low-carbon version, IN-738LC, in the form of cast-to-shape test bars, Figure 3.044.
3.045	Creep-rupture curve at 1560 F for the low-carbon version, IN-738LC, in the form of cast-to-size specimens and specimens machined from blades, Figure 3.045.
3.046	Creep-rupture strength of regular and low-carbon grades of IN-738 for various temperatures and rupture times, Figure 3.046.
3.047	Creep-rupture properties at various temperatures and stresses, Table 3.047.
3.048	Comparison of some creep-rupture properties of as-cast and heat-treated, cast-to-size test specimens, Table 3.048.
3.049	Creep-rupture life of the low-carbon version, IN-738LC, at 1560 F after various exposures at 1560 F in air with no load, Figure 3.049.
3.0410	Effects of prior exposures for 200 hr at 1850 F in various environments on creep-rupture life determined in air at various stresses and at temperatures from 1290 to 1850 F, Figure 3.0410.
3.0411	Effects of prior exposures for 200 hr at 1850 F in air on creep-rupture life of bare and coated specimens determined in air at various stresses and temperatures from 1290 to 1850 F., Figure 3.0411.
3.0412	Effects of prior long-term exposures in air at 1560 and 1740 F on creep-rupture time and ductility of specimens tested at 1550 F and 50 ksi, Figure 3.0412.
3.0413	Effects of prior exposures in air at 1650, 1830, and 2010 F on creep-rupture time and ductility of specimens tested at 1470 F and 58 ksi, Figure 3.0413.
3.0414	Effect of prior cycling between 750 and 1830 F in air on creep-rupture life at 1600 F and 40 ksi, Figure 3.0414.
3.0415	Effects of coating specimens with various amounts of sea salt prior to testing on relative creep-rupture life in air, Table 3.0415.
3.0416	Bar graph representing creep-rupture time and ductility at various temperatures and stresses for directionally solidified IN-738 in orientations parallel to (L), perpendicular to (T), and diagonal to (D) the solidification direction, Figure 3.0416.
3.0417	Effects of interrupting creep exposures for reheat treatment on total creep-rupture time at two levels of stress and temperature, Table 3.0417.

Ni
16 Cr
8.5 Co
3.5 Al
3.5 Ti
2.6 W
1.8 Mo
0.9 Cb

IN-738

Ni
16 Cr
8.5 Co
3.5 Al
3.5 Ti
2.6 W
1.8 Mo
0.9 Cb

IN-738

3.0418 Effects of hot isostatic pressing (HIP) on creep-rupture properties at 1800 F and 22 ksi of specimens cast to size and machined from cast slabs, Table 3.0418.

3.05 Fatigue Properties

3.051 Fatigue life as a function of maximum cyclic stress at temperatures up to 1700 F, Figure 3.051.

3.052 Fatigue life of the low-carbon version, IN-738LC, as a function of maximum cyclic stress at temperatures from 1290 F to 1650 F, Figure 3.052.

3.053 Fatigue life at 1600 F as a function of the total cyclic strain range for various types of cycling, Figure 3.053.

3.054 Effects of prior exposures to elevated temperatures in air and vacuum on fatigue life in air at 1560 F, Figure 3.054.

3.055 Effects of prior exposure to hot-corrosive environment on fatigue life in air at 1560 F, Figure 3.055.

3.056 Effects of strain rate and hot-corrosive conditions on fatigue life as a function of cyclic plastic strain range at 1650 F, Figure 3.056.

3.057 Stress-range diagram for the low-carbon version, IN-738LC, showing the effect of hot isostatic pressing (HIP) on combinations of mean and alternating stresses required to cause fatigue failure in 10^8 cycles at 1200 F, Figure 3.057.

3.058 Effects of variations in stress intensity range and stress ratio on fatigue crack-growth rate at room temperature, Figure 3.058.

3.059 Effects of variations in stress intensity range and temperature on fatigue crack-growth rate, Figure 3.059.

3.0510 Effects of variations in stress intensity range and of long-term exposure at 1560 F in air on fatigue crack-growth rate at room temperature, Figure 3.0510.

3.0511 Effects of variations in stress intensity range and of long-term exposure at 1560 F in air on fatigue crack-growth rate at 1560 F, Figure 3.0511.

3.0512 Effects of variations in stress intensity range and orientation on fatigue crack-growth rate at room temperature in directionally solidified castings, Figure 3.0512.

3.0513 Effects of variations in stress intensity range and orientation on fatigue crack-growth rate at 1560 F in directionally solidified castings, Figure 3.0513.

3.0514 Fatigue crack-growth rate as a function of stress intensity range in air and vacuum at 1560 F, Figure 3.0514.

3.0515 Effect of cycling frequency and stress intensity range on fatigue crack-growth rate in air and vacuum, Figure 3.0515.

3.0516 Tests in which tapered-disc specimens were cycled at 2-minute intervals between fluidized beds at room temperature and an elevated temperature caused thermal-fatigue cracking to initiate in IN-738 at 1790, 150, and 13 cycles when the peak temperatures were 1470, 1650, and 1830 F, respectively. These thermal-fatigue chracteristics are comparable to those of 713C and IN-100 alloys (2).

3.06 Elastic Properties

3.061 Poisson's ratio.

3.0611 Poisson's ratio at temperatures from 75 F to 1800 F, Figure 3.0611.

3.062 Modulus of elasticity.

3.0621 Effect of elevated temperatures on modulus of elasticity, Figure 3.0621.

3.063 Modulus of rigidity.

3.0631 Effect of elevated temperatures on modulus of rigidity, Figure 3.0631.

3.064 Tangent modulus.

3.065 Secant modulus.

4 FABRICATION

4.01 Forming

IN-738 parts are formed by direct casting to shape from the liquid state. No hot or cold forming is carried out in the solid state, except that powder-metal parts have been produced experimentally. Castings can be finished by machining and grinding.

4.02 Machining and Grinding

4.021 The machinability of IN-738 is comparable to that of other nickel-base superalloys. With rigid machines and sturdy tools, it can be machined in either the as-cast or heat-treated condition with either carbide or high-speed tool-steel cutting tools. Low speeds and small positive feeds with no dwelling of the tool are necessary. Keenly ground tools free of feather edges and a continuous stream of lubricant are essential. Chemical emulsions and heavy-duty chlorinated mineral oil have been used successfully as lubricants. Parts should be thoroughly cleaned before they are exposed to elevated temperatures (2,43).

4.022 Grinding should be carried out preferably with light feeds, high speeds up to 6000 surface feet/minute, and continuous use of grinding fluid. Highly sulfurized oil is a satisfactory fluid providing it is thoroughly removed from the finished ground part. If not removed, the fluid causes discoloration at room temperature and hot corrosion at high temperatures (43).

4.023 As with other nickel-base alloys, electrical-discharge and electrochemical machining techniques are applicable to IN-738 (43).

4.03 Joining

4.031 IN-738 is generally considered to be unweldable by ordinary techniques because it is very sensitive to hot cracking during welding and to the formation of cracks in the weld metal and heat-affected zone during subsequent heat treatment. Recent research indicates that the susceptibility to cracking can be significantly reduced by welding with minimum heat input and speed, by using base metal with minimum impurity content, and by using ductile weld fillers. Using these welding techniques and subsequent hot isostatic pressing followed by conventional heat treatment, weld cracks can be eliminated and acceptable mechanical properties can be achieved in repair welds in IN-738 (2,44).

4.032 If preheated to 2050 F and conventionally heat treated after welding, IN-738 can be successfully electron-beam welded with or without the use of filler metal. The resulting welds have reasonably uniform hardness, strength, and fatigue properties approaching those of the base metal, but the ductility is somewhat erratic (39).

4.033 Brazing (see 713C, Code 4119, Section 4.032).

4.04 Surface Treating

4.041 Castings can be rough cleaned by sand or grit blasting, but for complete removal of investment mold material and oxide skin, it is usually necessary to immerse in one of the commercially available caustic-base salt baths and then to pickle in hot sulfuric and hot nitric-hydrofluoric acid.

4.042 A number of coatings have been developed and evaluated for the protection of IN-738 and other nickel-base superalloys against oxidation and hot corrosion. An aluminide type of coating has been the best established and most widely used. A relatively recent improvement has been the addition of a noble metal, platinum or rhodium, to the aluminide. These coatings are generally applied by chemical vapor deposition (pack cementation) or physical vapor deposition methods (plasma spray, ion implantation, sputtering, and electron-beam evaporation). The details of most of the commercial aluminizing processes are proprietary and the thickness, microstructure, morphology, and overall composition depend upon the process technology. A promising more recent development is a Co Cr Al Y type coating applied by electron-beam or vacuum-plasma deposition (Figure 3.0411). Coatings detract from mechanical properties to the extent that they involve diffusion into and interaction with the substrate, thereby reducing its effective load-bearing cross-sectional area. This effect can be appreciable with thin-wall components. The detrimental effects on mechanical properties are more pronounced with chemical vapor deposition than with physical vapor deposition (20,37,38).

4.0421 In heat-corrosion tests, in which IN-738 was exposed to sodium sulfate at 1800 F, corrosion products formed in about 175 hr. (See Figure 2.0333.) Application of various types of coatings, such as aluminide, platinum-aluminide, or Co Cr Al Y alloy, has more than doubled the time required for the formation of hot-corrosion products. The Co Cr Al Y coating was most effective, platinum-aluminide coating was next, and simple aluminide coating was least effective (16). Similar results on the relative effectiveness of the various types of coatings were obtained in burner-rig tests in which samples were cyclically exposed at 1750 F and 2100 F to a Mach 0.7 stream of gases created by burning JP-5 fuel. The same investigation showed vacuum-plasma-deposition coatings of Co Cr Al Y up to 0.006-inch thick to have only minor detrimental effects on fatigue properties (38).

REFERENCES

1 Schultz, J. W. and Hulsizer, W. R., "Corrosion-Resistant Nickel-Base Alloys for Gas Turbines", Metals Engineering Quarterly, 16 (August 1976) p 15-23.

2 "Alloy IN-738 Technical Data", The International Nickel Co., Inc., 15Cl-81 5789 (1981).

3 Merrick, H. F., Maxwell, D. H., and Gibson, R. C., "Fatigue in the Design of High-Temperature Alloys", Fatigue at Elevated Temperatures, ASTM STP520 (June 1972).

4 "A Quick Guide to the Nickel Containing Casting Alloys", The International Nickel Co., Inc., 10M 4-82 5864 (1982).

5 Stearns, C. A., Kohl, F. J., and Fryburg, G. C., "Susceptibility to Hot Corrosion of Four Nickel-Base Superalloys", NASA Lewis Research Center, NASA-TN-D-8461, N77-21216 (April 1977).

6 Metals Handbook, Ninth Edition, Vol. 3, American Society for Metals (1980).

7 Woodford, D. A. and Frawley, J. J., "The Effect of Grain-Boundary Orientation on Creep and Rupture of IN-738 and Nichrome", Metallurgical Transactions, 5 (September 1974) p 2005-2013.

8 Jackson, M. R. and Rairden, J. R., "The Aluminization of Platinum and Platinum-Coated IN-738", Metallurgical Transactions, 8A (November 1977) p 1697-1707.

9 Scarlin, R. B., "Fatigue Crack Growth in a Cast Ni-Base Alloy", Materials Science and Engineering, 21 (1975) p 139-147.

10 Scarlin, R. B., "Creep and Fatigue Crack Growth in Overaged Nickel-Base Alloys", Materials Science and Engineering, 30 (September 1977) p 55-64.

11 Scarlin, R. B., "Fatigue Crack Propagation in a Directionally Solidified Nickel-Base Alloy", Metallurgical Transactions, 7A (October 1976) p 1535-1541.

12 Steven R. A. and Flewitt, P.E.J., "Microstructural Changes Which Occur During Isochronal Heat Treatment of Nickel-Base Superalloy IN-738", Journal of Materials Science, 13 (February 1978) p 367-376.

13 Wigton, H. F., "Corrosion of Superalloys, Inconels, and Stainless Steels by the Products from Fluidized Bed Coal Combustion", Materials Performance, 17 (January 1978) p 31-43.

14 Ostergren, W. J., "A Damage Function and Associated Failure Equations for Predicting Hold Time and Frequency Effects in Elevated Temperature, Low Cycle Fatigue", Journal of Testing and Evaluation, 4 (September 1976) p 327-339.

15 Shaw, S.W.K., "IN-939: A Corrosion-Resistant Alloy for Industrial and Marine Turbine Blades", Metal Progress, 115 (March 1979) p 47-50.

16 Patarini, V., Bornstein, N. S., and DeCrescente, M. A., "Hot Corrosion of Gas Turbine Components", Transactions ASME, Journal of Engineering for Power, 101 (January 1979) p 177-185.

Ni
16 Cr
8.5 Co
3.5 Al
3.5 Ti
2.6 W
1.8 Mo
0.9 Cb
IN-738

Ni
16 Cr
8.5 Co
3.5 Al
3.5 Ti
2.6 W
1.8 Mo
0.9 Cb

IN-738

17 Frawley, J. J., Moore, W. F., and Kiesler, A. J., "Solidification Under Pressure Greater than Atmospheric", AFS International Cast Metals Journal, 5 (September 1980) p 31-39.

18 Just, C. and Franklin, C. A., "Evaluation Program for New Industrial Gas Turbine Materials", Transactions ASME, Journal of Engineering for Power, 100 (October 1978) p 704-711.

19 Stevens, R. A. and Flewitt, P.E.J., "The Effects of Gamma Prime Precipitate Coarsening During Isothermal Aging and Creep of the Nickel-Base Superalloy IN-738", Materials Science and Engineering, 37 (March 1979) p 237-247.

20 Restall, J. E., "High Temperature Coatings for Protecting Hot Components in Gas Turbine Engines", Metallurgia, 46 (November 1979) p 676-685.

21 "Description and Engineering Characteristics of Eleven New High-Temperature Alloys", DMIC Memorandum 255, Battelle's Columbus Laboratories (June 1971).

22 "Preliminary Properties of IN-738 Alloy", DMIC Technical Note, Battelle's Columbus Laboratories (March 15, 1970).

23 Wasielewski, G. E. and Linblad, "Elimination of Casting Defects Using HIP", Superalloys Processing, Proceedings of the Second International Conference, The Metallurgical Society AIME, MCIC 72-10 (September 1972).

24 Bieber, C. G. and Michalisin, J. R., "Structural Studies and Properties of a New Cast High-Strength Corrosion-Resistant Superalloy", Second International Conference on the Strength of Metals and Alloys, American Society for Metals, Metals Park, Ohio (1970).

25 Susukida, H., et al., "Strength and Microstructure of Nickel-Base Superalloys after Long-Term Heating", Mitsubishi Heavy Industries, MTB86 (May 1973).

26 Hart, A. B. and Cutler, A.J.B., "An Evaluation of the Hot Corrosion Resistance of Commercial High-Chromium Nickel-Base Alloys for Use in Gas Turbines", Deposition and Corrosion in Gas Turbines, John Wiley & Sons (1973).

27 Lowell, C. E. and Probst, H. B., "Effects of Composition and Testing Conditions on Oxidation Behavior of Four Cast Commercial Nickel-Base Superalloys", NASA TN D-7705 (August 1974).

28 Stearns, C. A., Kohl, F. J., and Fryburg, G. C., "Susceptibility to Hot Corrosion of Four Nickel-Base Superalloys, NASA-TRW VIA, B-1900, 713C, and IN-738", NASA TN D-8461 (April 1977).

29 Woodford, D. A., "The Effect of Prior Temperature Cycling on Rupture Life of Superalloys", Proceedings of the Fourth International Conference on Fracture, University of Waterloo Press (June 19-24, 1977) p 802-812.

30 Scarlin, R. B., "Effects of Loading Frequency and Environment on High-Temperature Fatigue Crack Growth in Nickel-Base Alloys", Proceedings of the Fourth International Conference on Fracture, University of Waterloo Press (June 19-24, 1977) p 849-853.

31 McColvin, G. M., "High Cycle Fatigue of Nickel-Base Alloys", Henry Wiggins & Co., Ltd., Technical Report 2977 (June 1977).

32 Van Drunen, G., et al., "Hot Isostatic Pressing of IN-738 Turbine Blades", Proceedings of the 47th Meeting of the AGARD Structures and Materials Panel, Florence, Italy (September 1978) p 13-1/13-12.

33 Woodford, D. A. and Bricknell, R. H., "The Effect of High Temperature Air Exposure on the Stress Rupture Life of Nickel and Cobalt Base Superalloys", Proceedings of the Fourth International Symposium on Superalloys, AIME and ASM (September 1980) p 633-641.

34 Stevens, R. A. and Flewitt, P.E.J., "Regenerative Heat Treatments for the Extension of the Creep Life of the Superalloy IN-738", International Conference on the Strength of Metals and Alloys, Aachen, Germany (August 1979) p 439-444.

35 Galsworthy, J. C., "The Effects of Sea Salt on the High-Temperature Creep Properties of a Nickel Base Gas Turbine Blade Alloy", Corrosion and Mechanical Stress at High Temperatures", Applied Science Publishers, Essex, England (May 1980) p 197-206.

36 Hoffelner, W. and Speidel, M. O., "Microstructural Aspects of Fatigue Crack Propagation of Cast Nickel-Base Superalloys at 850 C in Various Environments", Proceedings on Corrosion and Mechanical Stress at High Temperature, Applied Science Publishers, Essex, England (May 1980) p 275-287.

37 Woodford, D. A., "Environmental Damage of a Cast Nickel-Base Superalloy", Metallurgical Transactions, 12A (February 1981) p 299-308.

38 Shankar, S., Koenig, D. E., and Dardi, L. E., "Vacuum Plasma Sprayed Metallic Coatings", Journal of Metals, 33 (October 1981) p 13-20.

39 Jahnke, B., "High-Temperature Electron Beam Welding of the Nickel-Base Superalloy IN-738LC", Welding Journal, Research Supplement, 61 (November 1982) p 343S-347S.

40 Nazmy, M. Y., "The Effect of Environment on the High Temperature Low Cycle Fatigue Behavior of Cast Nickel-Base IN-738 Alloy", Materials Science and Engineering, 52 (September 1982) p 231-237.

41 Jianting, G., Ranucci, D., and Picco, E., "Low Cycle Fatigue Behavior of Cast Nickel-Base Superalloy IN-738LC in Air and in Hot Corrosive Environment", Materials Science and Engineering, 58 (March 1983) p 127-133.

42 Wilhem, D. P., "Standard Designation Code for Fracture Specimens, Loading, and Orientation", ASTM Standardization News (May 1982).

43 "Machining and Grinding IN-738 Alloy", The International Nickel Co., Inc., A-609 (1972).

44 Elsner, W., "Scope for Repair Welding Gas Turbine Blades", Practical Metallography, 19 (April 1982) p 199-206, 211-214.

45 Nazmy, M. Y., "The Effects of Sulfur Containing Environment on the High-Temperature Low Cycle Fatigue of a Cast Nickel-Base Alloy", Scripta Metallurgica, 16 (December 1982) p 1329-1332.

Alloy	IN-738	
Form	Cast	
	Percent	
Composition	Min	Max
C	0.15	0.20
Co	8.00	9.00
Cr	15.70	16.30
Mo	1.50	2.00
W	2.40	2.80
Ta	1.50	2.00
Cb	0.60	1.10
Al	3.20	3.70
Ti	3.20	3.70
Al+Ti	6.50	7.20
B	0.005	0.015
Zr	0.05	0.15
Fe	–	0.05
Mn	–	0.02
Si	–	0.03
S	–	0.015
Ni	Balance	

Note: For the low-carbon version, IN-738LC, the following modifications are specified: carbon = 0.09-0.13, boron = 0.007-0.012, and zirconium = 0.03-0.08.

TABLE 1.04. COMPOSITION(2)

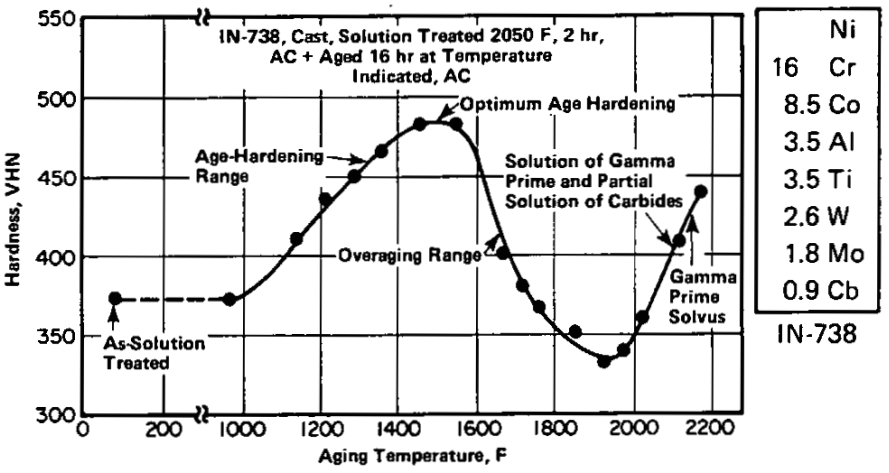

FIGURE 1.061. EFFECTS OF AGING FOR 16 HR AT VARIOUS ELEVATED TEMPERATURES ON HARDNESS OF SOLUTION-TREATED MATERIAL AT ROOM TEMPERATURE (12)

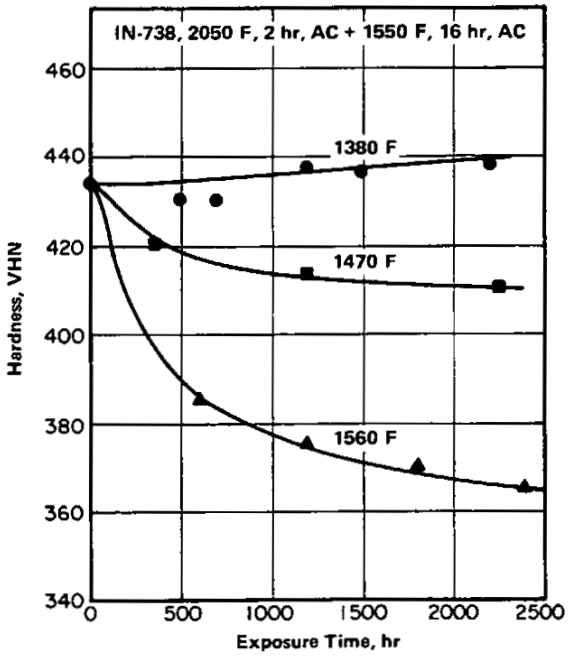

FIGURE 1.062. EFFECTS OF LONG-TIME EXPOSURES TO TEMPERATURES FROM 1380 TO 1560 F ON HARDNESS AT ROOM TEMPERATURE (19)

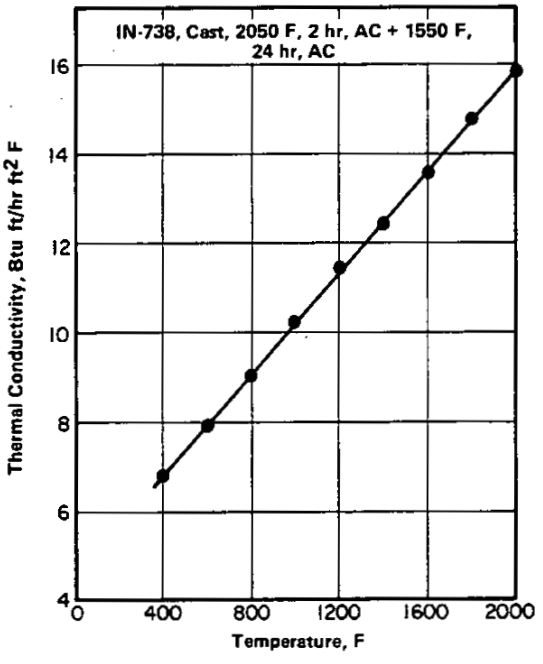

FIGURE 2.013. THERMAL CONDUCTIVITY (2)

Ni
16 Cr
8.5 Co
3.5 Al
3.5 Ti
2.6 W
1.8 Mo
0.9 Cb

IN-738

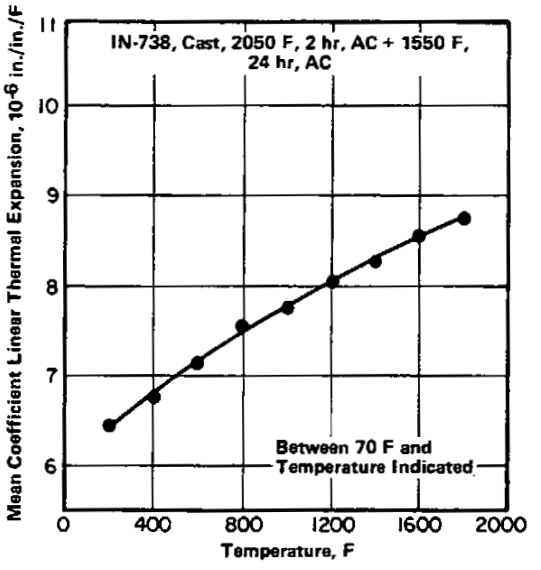

FIGURE 2.014. THERMAL EXPANSION (2)

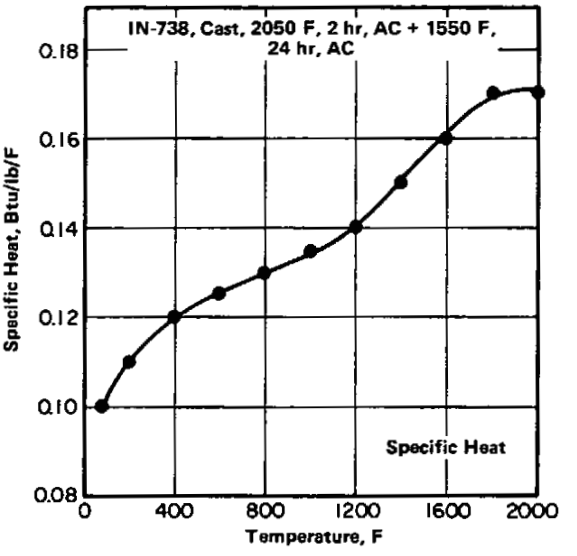

FIGURE 2.015. SPECIFIC HEAT (2)

Alloy	IN-738		
Form	Cast		
Condition	2050 F, 2 hr, AC + 1550 F, 24 hr, AC		
Oxidation Test: Exposed 400 hr at 2000 F to Air with 3 percent H_2O		Hot Corrosion Test: Exposed 300 hr at 1700 F to 90 percent Na_2SO_4 and 10 percent NaCl	
Descaled Weight Loss, mg/mm^2		Maximum Depth of Hot Corrosion, mm	
713C	IN-738	713C	IN-738
19	48	>7	1.2

TABLE 2.0311. COMPARISON OF THE RESISTANCE OF IN-738 AND 713C TO OXIDATION AND TO HOT CORROSION(3)

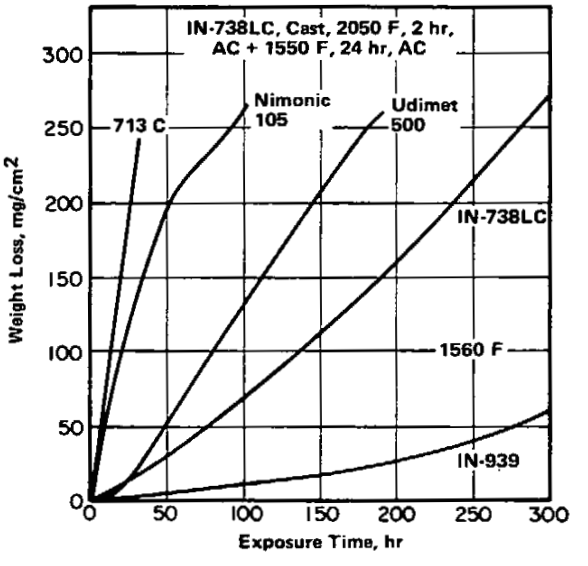

FIGURE 2.0332. EFFECTS OF EXPOSURE TIME ON WEIGHT LOSS DUE TO HOT CORROSION OF IN-738LC AND FOUR OTHER NICKEL-BASE SUPERALLOYS CAUSED BY EXPOSURES TO A CONTINUOUS SALT SHOWER OF 75 PERCENT SODIUM SULFATE AND 25 PERCENT SODIUM CHLORIDE AT 1560 F (15)

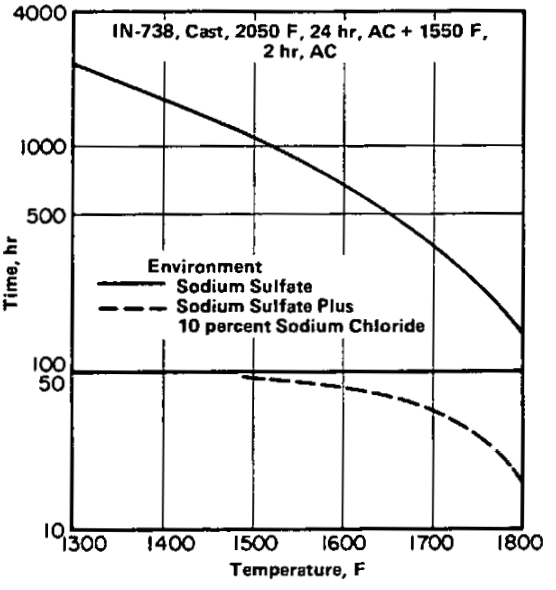

FIGURE 2.0333. EFFECT OF EXPOSURE TEMPERATURE ON TIME TO FORMATION OF VISIBLE HOT-CORROSION PRODUCTS IN ENVIRONMENTS OF SODIUM SULFATE AND OF SODIUM SULFATE PLUS 10 PERCENT SODIUM CHLORIDE (16)

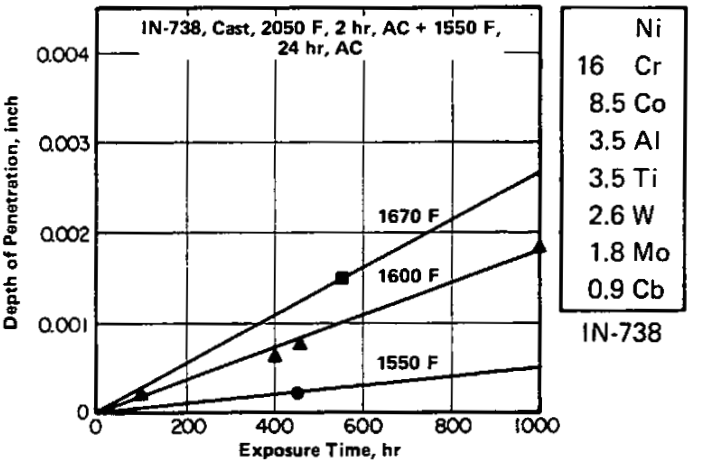

FIGURE 2.0334. EFFECTS OF TIME AND TEMPERATURE ON DEPTH OF PENETRATION OF HOT CORROSION AT ATMOSPHERIC PRESSURE IN COMBUSTION GASES FROM HIGH-SULFUR COAL TREATED WITH DOLOMITE AS A SULFUR SUPPRESSANT (13)

Alloy	IN-738	
Form	Cast	
Condition	2050 F, 2 hr, AC + 1550 F, 24 hr, AC	
Tensile Properties	IN-738, 0.17% C	IN-738LC, 0.11% C
F_{ty}, ksi	138	130
F_{tu}, ksi	159	150
e (2-inch), percent	5.5	7.0
RA, percent	5.0	9.0

TABLE 3.0211. COMPARISON OF ROOM-TEMPERATURE TENSILE PROPERTIES OF REGULAR AND LOW-CARBON GRADES OF IN-738 PRODUCED IN THE FORM OF CAST-TO-SIZE SPECIMENS(2)

Alloy	IN-738							
Form	Cast							
	Casting Configuration							
	Slab, 1x4x5 inch				Cast-to-Size Specimen			
Casting Condition	F_{ty}, ksi	F_{tu}, ksi	e (4D), percent	RA, percent	F_{ty}, ksi	F_{tu}, ksi	e (4D), percent	RA, percent
a	90	112	3.0	8.0	130	150	6.0	9.0
b	105	131	6.3	14.0	109	153	7.5	12.0
c	106	130	4.7	9.6	122	165	7.5	10.5

Note: a = cast + 2050 F, 2 hr, AC + 1550 F, 24 hr, AC
b = cast + HIP 2150 F, 2 hr at 14.5 ksi in argon, AC + 2150 F, 2 hr, AC
c = cast + HIP 2150 F, 2 hr at 14.5 ksi in argon, AC + 2150 F, 2 hr, AC + 2050 F, 2 hr, AC + 1550 F, 24 hr, AC.

TABLE 3.0212. EFFECTS OF HOT ISOSTATIC PRESSING (HIP) ON TENSILE PROPERTIES AT ROOM TEMPERATURE OF SPECIMENS CAST TO SIZE AND MACHINED FROM CAST SLABS(23)

Alloy	IN-738				
Form	Cast				
Condition	2500 F, 2 hr, AC + 1550 F, 24 hr, AC				
Mold Material	Freezing Pressure Atmospheres	F_{ty}, ksi	F_{tu}, ksi	e (4D), percent	RA, percent
Hot Ceramic, Slow Freezing	1	104.2	107.8	3.0	5.6
	10	111.5	120.0	5.0	8.0
Chilled Copper, Fast Freezing	1	113.5	152.0	10.0	9.4
	10	116.4	155.4	8.0	13.0

Note: Casting made in ceramic molds are slabs, 1x4x5 inch; castings made in chill molds are bars, 2x2x6 inch.

TABLE 3.0213. TENSILE PROPERTIES AFTER VACUUM MELTING AND THEN CASTING IN ONE AND TEN ATMOSPHERES OF ARGON INTO TWO TYPES OF MOLDS PROVIDING SLOW AND FAST FREEZING(17)

Ni
16 Cr
8.5 Co
3.5 Al
3.5 Ti
2.6 W
1.8 Mo
0.9 Cb

IN-738

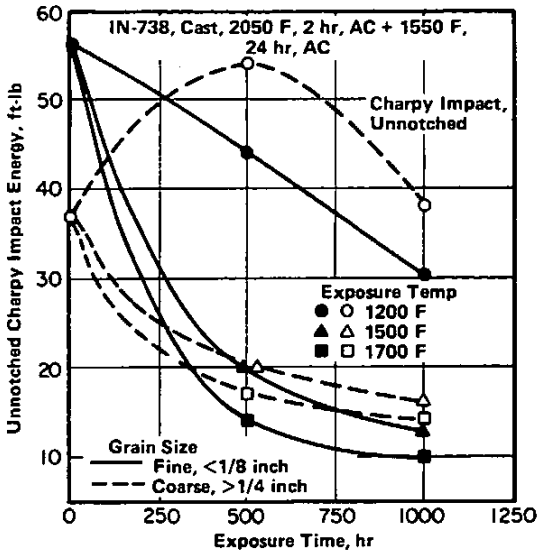

FIGURE 3.0231. EFFECTS OF EXPOSURE TO ELEVATED TEMPERATURES IN AIR ON UNNOTCHED CHARPY IMPACT STRENGTH OF FINE-GRAIN AND COARSE-GRAIN CASTINGS AT ROOM TEMPERATURE (2)

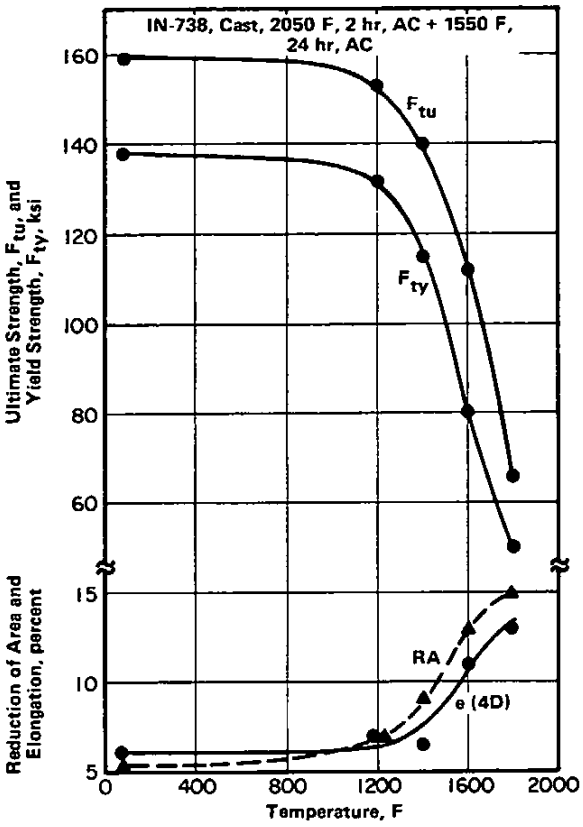

FIGURE 3.0311. TENSILE PROPERTIES OF CAST-TO-SIZE AND HEAT-TREATED TEST BARS IN THE TEMPERATURE RANGE 75 TO 1800 F (2)

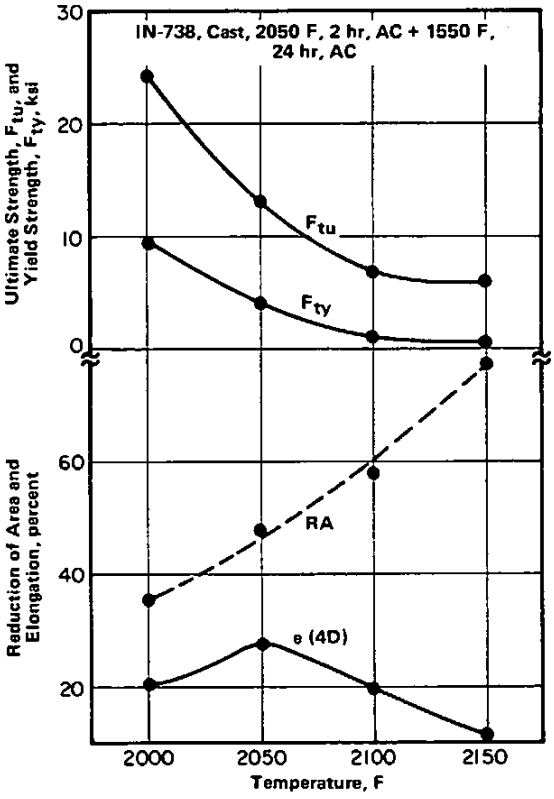

FIGURE 3.0312. TENSILE PROPERTIES OF CAST-TO-SIZE AND HEAT-TREATED TEST SPECIMENS AT TEMPERATURES FROM 2000 TO 2150 F (23)

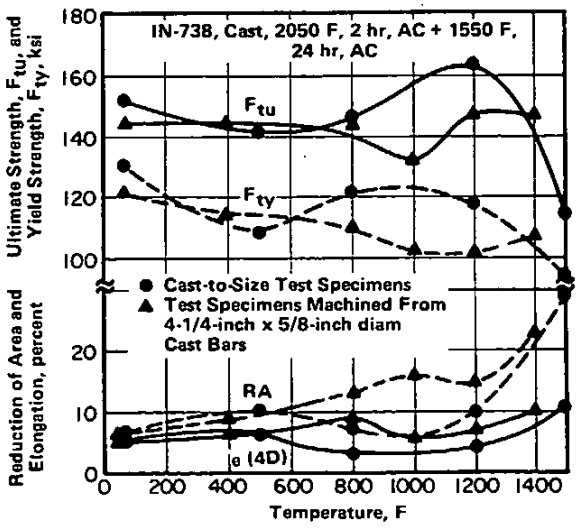

FIGURE 3.0313. EFFECTS OF TEMPERATURES UP TO 1500 F ON TENSILE PROPERTIES OF CAST-TO-SIZE SPECIMENS AND MACHINED SPECIMENS (22)

Ni
16 Cr
8.5 Co
3.5 Al
3.5 Ti
2.6 W
1.8 Mo
0.9 Cb

IN-738

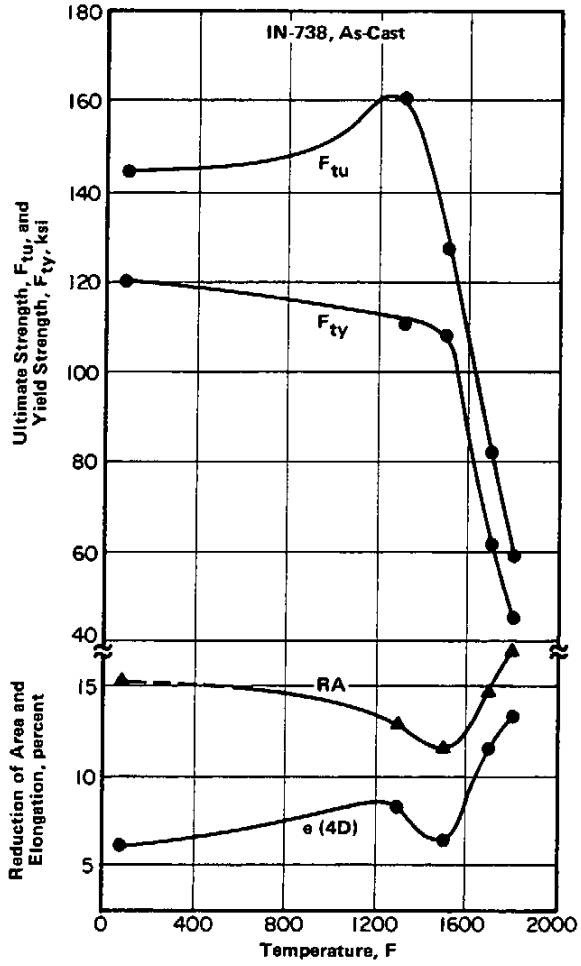

FIGURE 3.0314. TENSILE PROPERTIES OF AS-CAST, CAST-TO-SIZE TEST BARS IN THE TEMPERATURE RANGE 75 TO 1800 F (22)

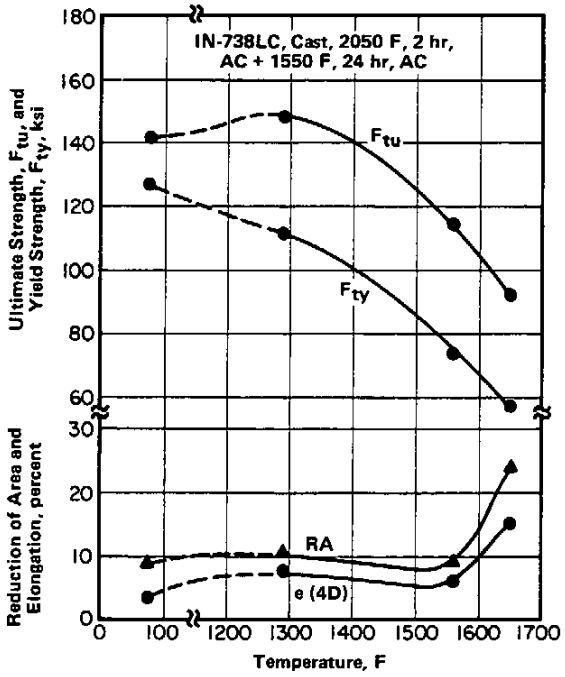

FIGURE 3.0315. TENSILE PROPERTIES OF THE LOW-CARBON VERSION, IN-738LC, IN THE FORM OF CAST-TO-SHAPE AND HEAT-TREATED TEST BARS AT TEMPERATURES UP TO 1650 F (31)

Ni
16 Cr
8.5 Co
3.5 Al
3.5 Ti
2.6 W
1.8 Mo
0.9 Cb

IN-738

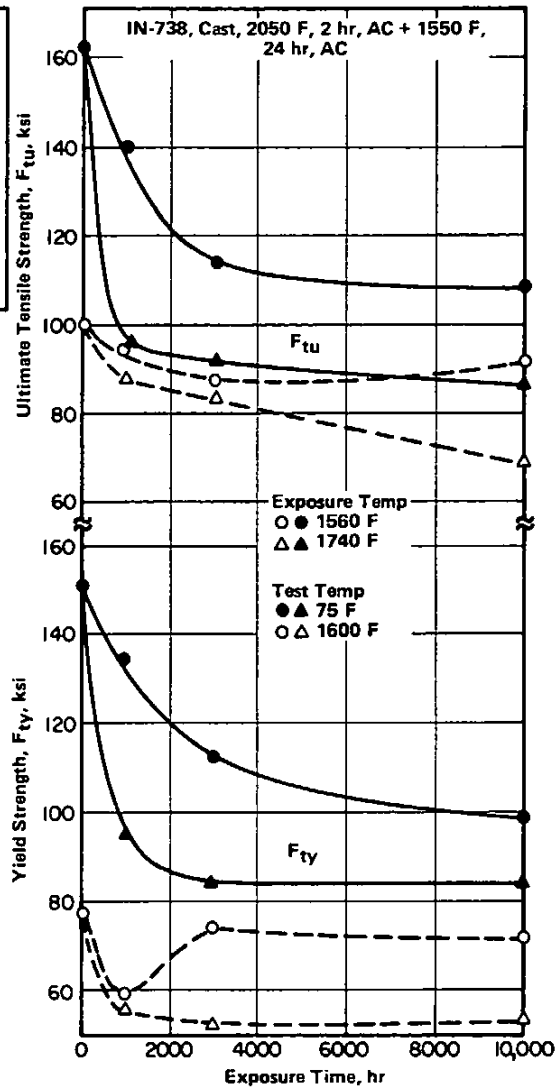

FIGURE 3.0316. EFFECTS OF LONG-TIME EXPOSURES IN AIR AT 1560 AND 1740 F ON TENSILE AND YIELD STRENGTHS OF SPECIMENS TESTED AT ROOM TEMPERATURE AND 1600 F (25)

Alloy	IN-738LC				
Form	Cast				
Casting Condition	Test Temp, F	F_{ty}, ksi	F_{tu}, ksi	e (4D), percent	RA, percent
a	77	113	133	6.9	8.5
b	77	122	139	5.7	13.0
a	1200	96	136	8.3	10.6
b	1200	103	143	8.9	13.3

Note: Test specimens machined from cast turbine blades.
a = cast + 2050 F, 2 hr, AC + 1550 F, 24 hr, AC
b = cast + HIP 2190 F, 2 hr at 14.5 ksi in argon, FC to 2050 F, hold 2 hr, AC + 1550 F, 24 hr, AC.

TABLE 3.0317. EFFECTS OF HOT ISOSTATIC PRESSING (HIP) ON TENSILE PROPERTIES OF THE LOW-CARBON VERSION, IN-738LC, AT ROOM TEMPERATURE AND 1200 F(32)

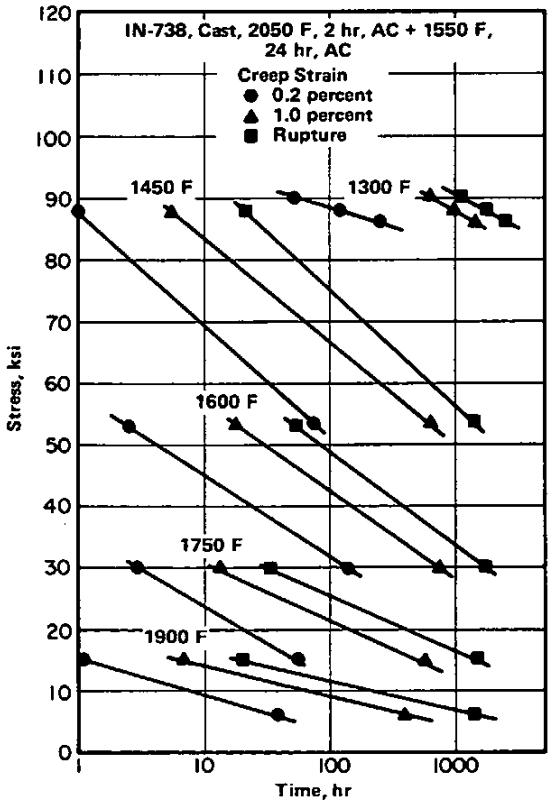

FIGURE 3.041. CREEP-DEFORMATION AND RUPTURE CURVES AT TEMPERATURES FROM 1300 TO 1900 F (22)

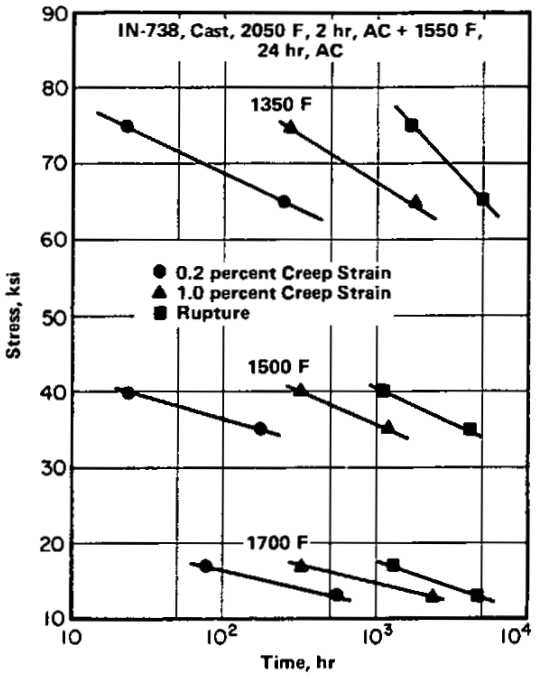

FIGURE 3.042. CREEP-DEFORMATION AND RUPTURE CURVES AT 1350, 1500, AND 1700 F (2)

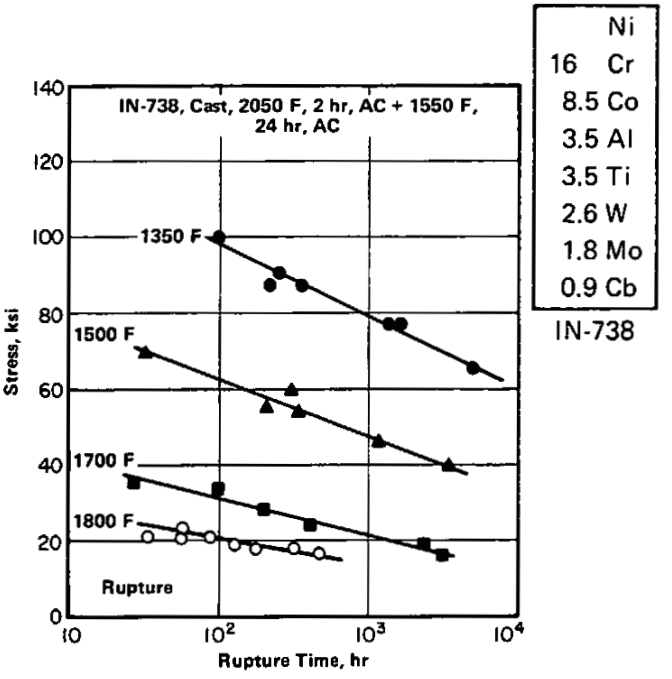

FIGURE 3.043. CREEP-RUPTURE CURVES AT TEMPERATURES FROM 1350 TO 1800 F (2, 21)

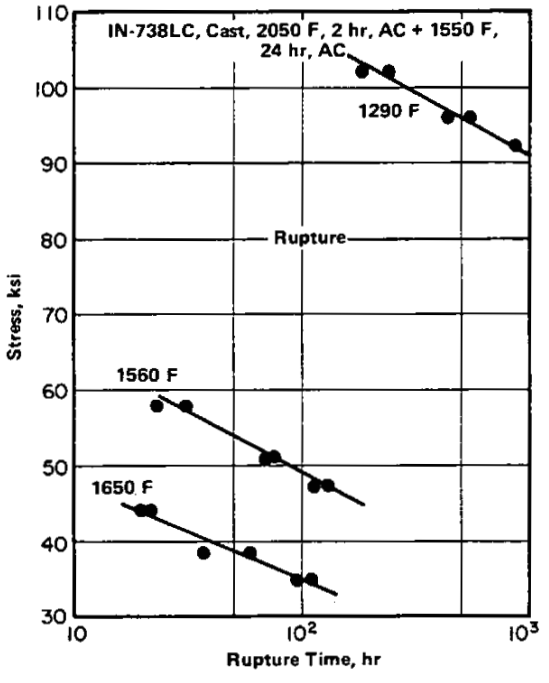

FIGURE 3.044. CREEP-RUPTURE CURVES AT TEMPERATURES FROM 1290 TO 1650 F FOR THE LOW-CARBON VERSION, IN-738LC, IN THE FORM OF CAST-TO-SHAPE TEST BARS (31)

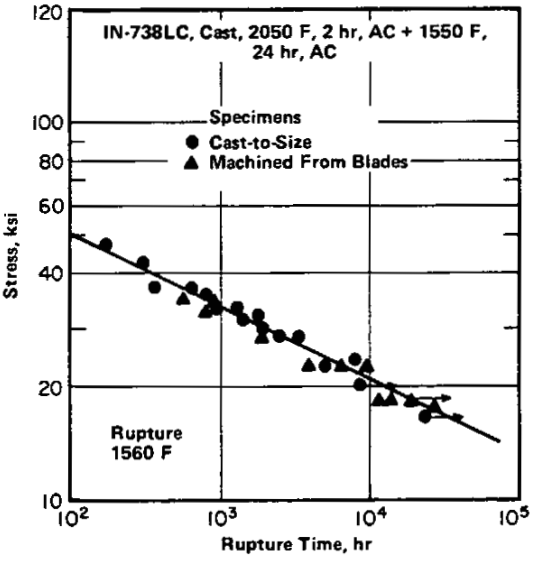

FIGURE 3.045. CREEP-RUPTURE CURVE AT 1560 F FOR THE LOW-CARBON VERSION, IN-738LC, IN THE FORM OF CAST-TO-SIZE SPECIMENS AND SPECIMENS MACHINED FROM BLADES (18)

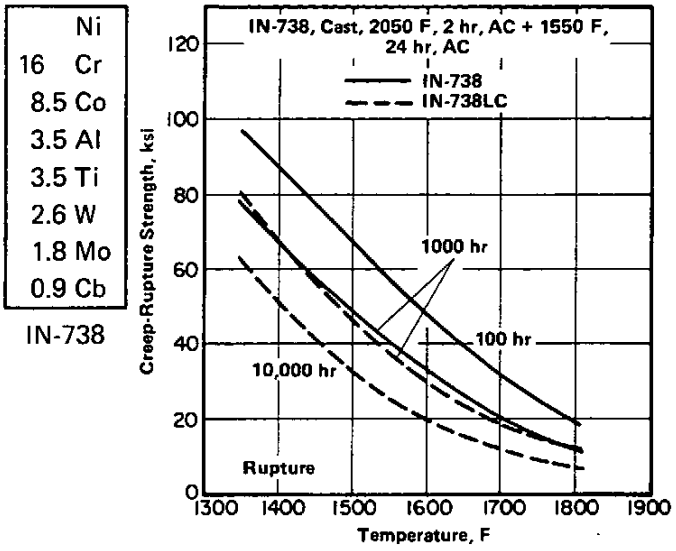

FIGURE 3.046. CREEP-RUPTURE STRENGTH OF REGULAR AND LOW-CARBON GRADES OF IN-738 FOR VARIOUS TEMPERATURES AND RUPTURE TIMES (2)

Alloy	IN-738			
Form	Cast			
Condition	2050 F, 2 hr, AC + 1550 F, 24 hr, AC			
Temp, F	Stress, ksi	Rupture Time, hr	e (4D), percent	RA, percent
1350	80	452	4	6
1350	90	211	6	9
1350	100	93	13	20
1400	90	89	4	8
1450	60	976	4	5
1500	40	3205	5	6
1500	55	261	11	14
1500	70	29	14	17
1600	40	371	9	13
1700	33	104	8	13
1700	35	29	15	17
1800	18	116	24	27
1800	22	48	14	23
1825	16	148	6	14

TABLE 3.047. CREEP-RUPTURE PROPERTIES AT VARIOUS TEMPERATURES AND STRESSES(2,21,22)

Alloy	IN-738				
Form	Cast				
Condition	Temp, F	Stress, ksi	Rupture Time, hr	e (4D), percent	RA, percent
As-Cast	1350	100	17.5	2.0	1.6
Heat-Treated	1350	100	93	13.0	20.0
As-Cast	1350	90	215	5.0	9.3
Heat-Treated	1350	90	211	6.0	9.0
As-Cast	1500	55	185	3.0	3.2
Heat-Treated	1500	55	261	11.0	14.0
As-Cast	1700	33	59	10.5	6.8
Heat-Treated	1700	33	104	8.0	13.0
As-Cast	1800	25	23.7	13.0	12.3
Heat-Treated	1800	25	55	6.0	–

Note: Heat treatment, 2050 F, 2 hr, AC + 1550 F, 24 hr, AC.

TABLE 3.048. COMPARISON OF SOME CREEP-RUPTURE PROPERTIES OF AS-CAST AND HEAT-TREATED, CAST-TO-SIZE TEST SPECIMENS(21,22)

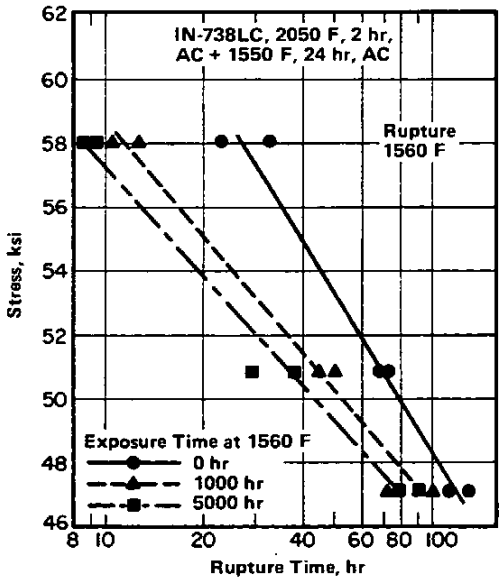

FIGURE 3.049. CREEP-RUPTURE LIFE OF THE LOW-CARBON VERSION, IN-738LC, AT 1560 F AFTER VARIOUS EXPOSURES AT 1560 F IN AIR WITH NO LOAD (31)

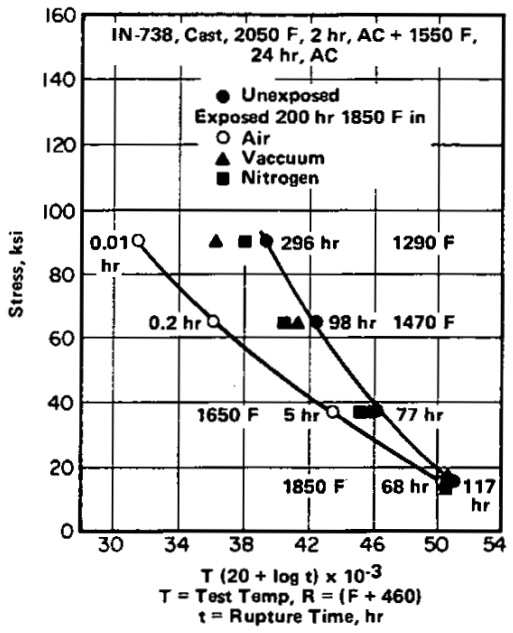

	Ni
16	Cr
8.5	Co
3.5	Al
3.5	Ti
2.6	W
1.8	Mo
0.9	Cb

IN-738

FIGURE 3.0410. EFFECTS OF PRIOR EXPOSURES FOR 200 HR AT 1850 F IN VARIOUS ENVIRONMENTS ON CREEP-RUPTURE LIFE DETERMINED IN AIR AT VARIOUS STRESSES AND AT TEMPERATURES FROM 1290 TO 1850 F (33)

The data are shown in terms of the Larson-Miller-time-temperature parameter, but for each combination of stress and temperature the shortest and longest rupture times are indicated.

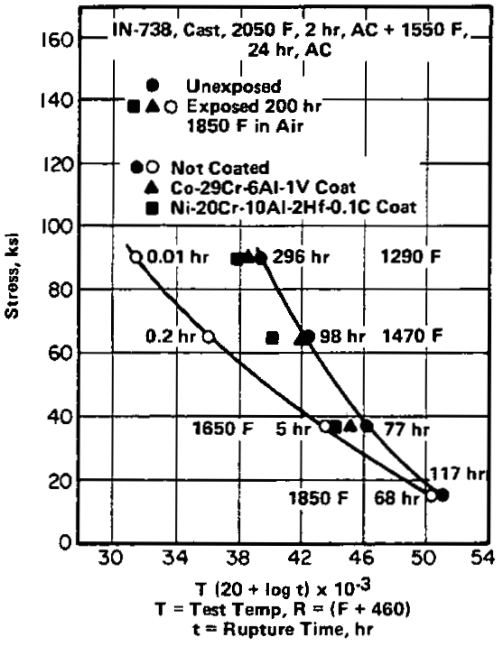

FIGURE 3.0411. EFFECTS OF PRIOR EXPOSURES FOR 200 HR AT 1850 F IN AIR ON CREEP-RUPTURE LIFE OF BARE AND COATED SPECIMENS DETERMINED IN AIR AT VARIOUS STRESSES AND TEMPERATURES FROM 1290 TO 1850 F (37)

The data are shown in terms of the Larson-Miller-time-temperature parameter, but for each combination of stress and temperature the shortest and longest rupture times are indicated. Coatings are approximately 0.005 in. thick and applied by vacuum plasma spray process.

Ni
16 Cr
8.5 Co
3.5 Al
3.5 Ti
2.6 W
1.8 Mo
0.9 Cb

IN-738

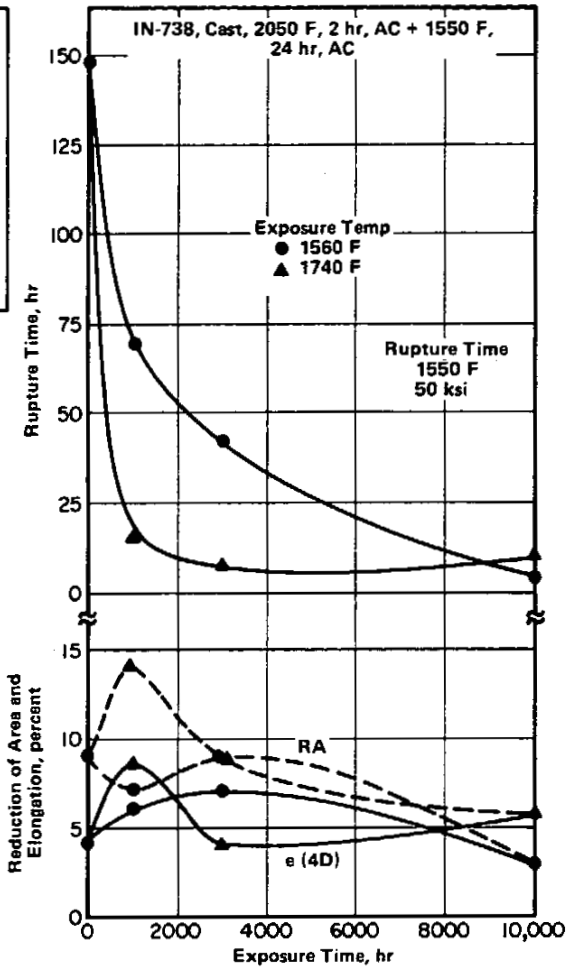

FIGURE 3.0412. EFFECTS OF PRIOR LONG-TIME EXPOSURES IN AIR AT 1560 AND 1740 F ON CREEP-RUPTURE TIME AND DUCTILITY OF SPECIMENS TESTED AT 1550 F AND 50 KSI (25)

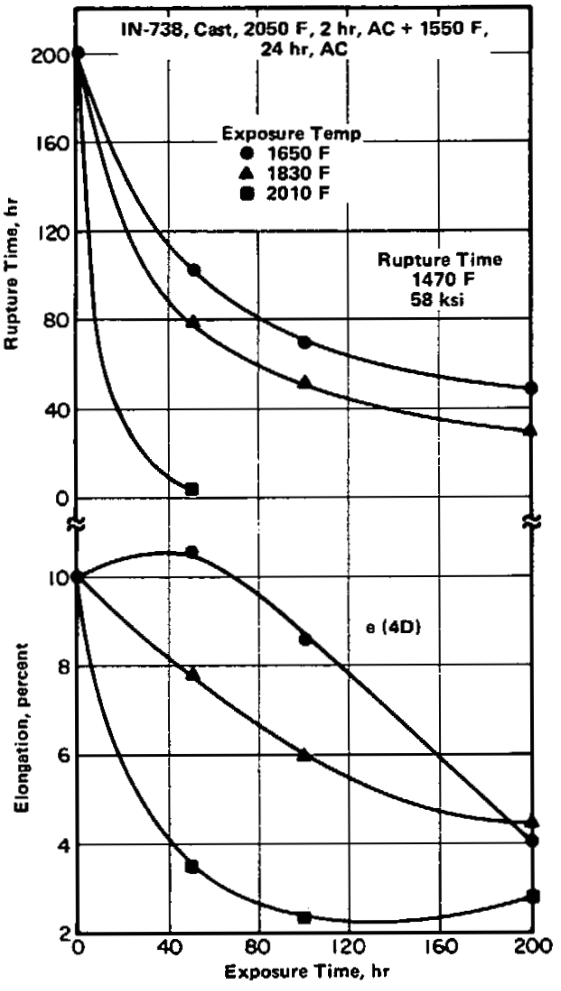

FIGURE 3.0413. EFFECTS OF PRIOR EXPOSURES IN AIR AT 1650, 1830, AND 2010 F ON CREEP-RUPTURE TIME AND DUCTILITY OF SPECIMENS TESTED AT 1470 F AND 58 KSI (37)

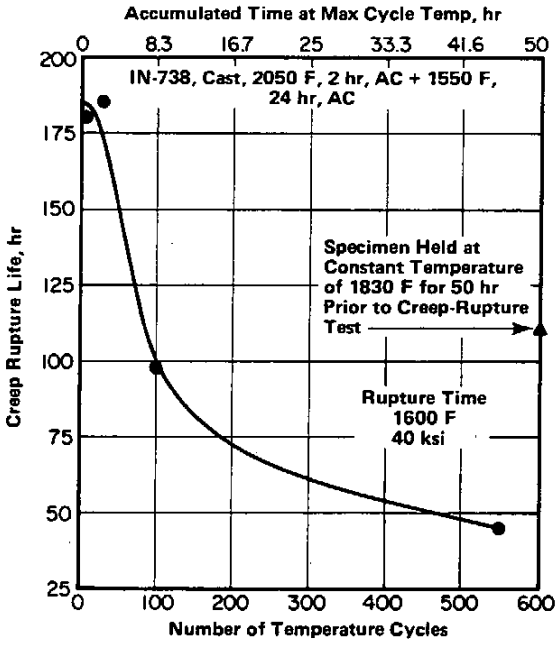

FIGURE 3.0414. EFFECT OF PRIOR CYCLING BETWEEN 750 F AND 1830 F IN AIR ON CREEP-RUPTURE LIFE AT 1600 F AND 40 KSI (29)

Each cycle lasted 15 minutes including a 5-minute hold at maximum temperature.

Alloy	IN-738				
Form	Cast				
Condition	2050 F, 2 hr, AC + 1550 F, 24 hr, AC				
		Percentage of Creep-Rupture Life of Uncoated Specimens for Specimens Coated With Sea Salt			
		Sea Salt Coatings, mg/mm^2			
Temp, F	Stress, ksi	None	0.02	0.10	1.0
1380	53.0	100	19	24.0	0.8
1470	43.5	100	58	20.0	0.3
1560	29.0	100	7	14.5	0.5

Note: Sea salt contained 6.5 percent sulfate ions, which along with sodium chloride are the active corrodants.

TABLE 3.0415. EFFECTS OF COATING SPECIMENS WITH VARIOUS AMOUNTS OF SEA SALT PRIOR TO TESTING ON RELATIVE CREEP-RUPTURE LIFE IN AIR(35)

Ni
16 Cr
8.5 Co
3.5 Al
3.5 Ti
2.6 W
1.8 Mo
0.9 Cb

IN-738

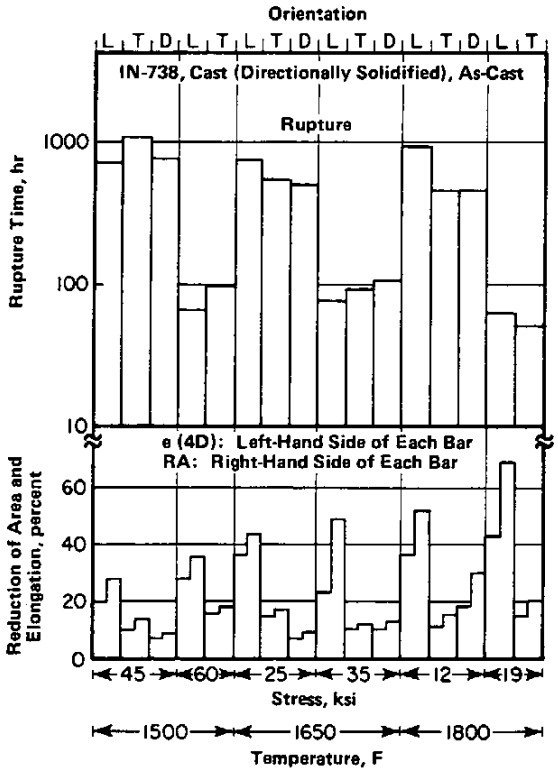

FIGURE 3.0416. BAR GRAPH REPRESENTING CREEP-RUPTURE TIME AND DUCTILITY AT VARIOUS TEMPERATURES AND STRESSES FOR DIRECTIONALLY SOLIDIFIED IN-738 IN ORIENTATIONS PARALLEL TO (L), PERPENDICULAR TO (T), AND DIAGONAL TO (D) THE SOLIDIFICATION DIRECTION (7)

Ni
16 Cr
8.5 Co
3.5 Al
3.5 Ti
2.6 W
1.8 Mo
0.9 Cb

IN-738

Alloy	IN-738		
Form	Cast		
Condition	2050 F, 2 hr, AC + 1550 F, 24 hr, AC		
Temp, F	Stress, ksi	Creep Time Before Reheat Treatment, hr	Rupture Time, hr
1380	66.3	Not Reheat Treated	1542
		764	1872
		1000	1844
		1250	1889
1560	35.4	Not Reheat Treated	1100
		358	1819
		650	1644
		811	1405

Note: Reheat treatment exactly the same as initial heat treatment given above.

TABLE 3.0417. EFFECTS OF INTERRUPTING CREEP EXPOSURES FOR REHEAT TREATMENT ON TOTAL CREEP-RUPTURE TIME AT TWO LEVELS OF STRESS AND TEMPERATURE(34)

Alloy	IN-738					
Form	Cast					
	Casting Configuration					
	Slab, 1x4x5 inch			Cast-to-Size Specimen		
Casting Condition	Rupture Time, hr	e (4D), percent	RA, percent	Rupture Time, hr	e (4D), percent	RA, percent
a	28	9	17	50	15	26
b	24	14	32	28	28	30
c	51	14	23	67	21	24

Note: a = cast + 2050 F, 2 hr, AC + 1550 F, 24 hr, AC
b = cast + HIP 2150 F, 2 hr at 14.5 ksi in argon, AC + 2150 F, 2 hr, AC
c = cast + HIP 2150 F, 2 hr at 14.5 ksi in argon, AC + 2150 F, 2 hr, AC + 2050 F, 2 hr, AC + 1550 F, 24 hr, AC.

TABLE 3.0418. EFFECT OF HOT ISOSTATIC PRESSING (HIP) ON CREEP-RUPTURE PROPERTIES AT 1800 F AND 22 KSI OF SPECIMENS CAST TO SIZE AND MACHINED FROM CAST SLABS(23)

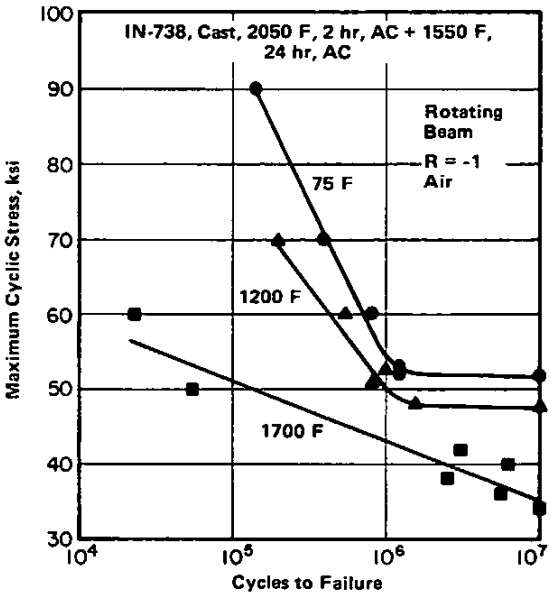

FIGURE 3.051. FATIGUE LIFE AS A FUNCTION OF MAXIMUM CYCLIC STRESS AT TEMPERATURES UP TO 1700 F (22)

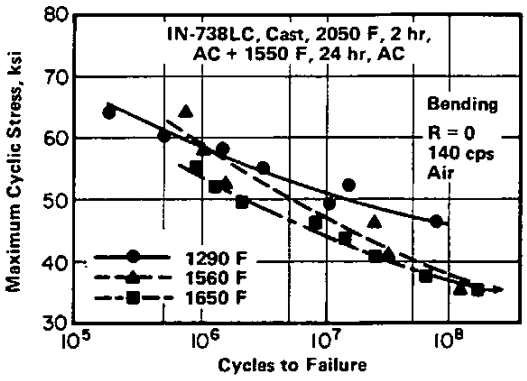

FIGURE 3.052. FATIGUE LIFE OF THE LOW-CARBON VERSION, IN-738LC, AS A FUNCTION OF MAXIMUM CYCLIC STRESS AT TEMPERATURES FROM 1290 F TO 1650 F (31)

	Ni
16	Cr
8.5	Co
3.5	Al
3.5	Ti
2.6	W
1.8	Mo
0.9	Cb

IN-738

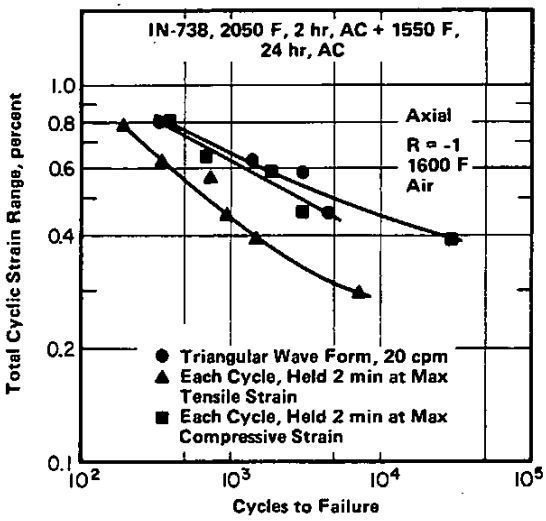

FIGURE 3.053. FATIGUE LIFE AT 1600 F AS A FUNCTION OF THE TOTAL CYCLIC STRAIN RANGE FOR VARIOUS TYPES OF CYCLING (14)

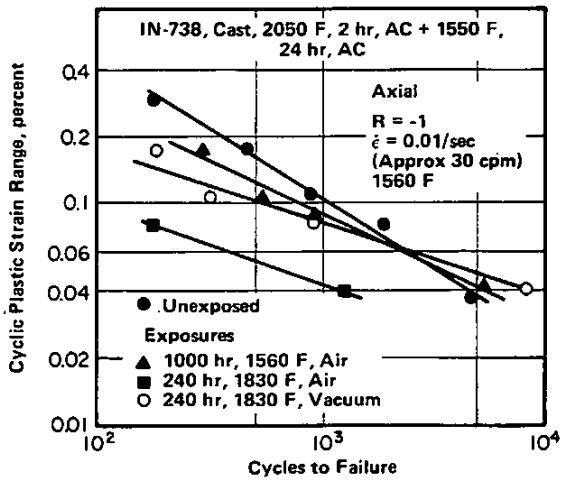

FIGURE 3.054. EFFECTS OF PRIOR EXPOSURES TO ELEVATED TEMPERATURES IN AIR AND VACUUM ON FATIGUE LIFE IN AIR AT 1560 F (40)

Ni
16 Cr
8.5 Co
3.5 Al
3.5 Ti
2.6 W
1.8 Mo
0.9 Cb

IN-738

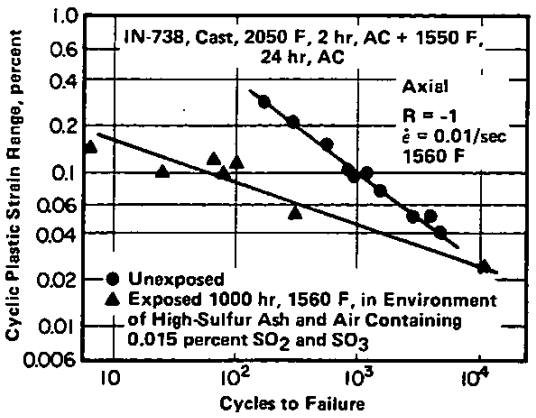

FIGURE 3.055. EFFECTS OF PRIOR EXPOSURE TO HOT-CORROSIVE ENVIRONMENT ON FATIGUE LIFE IN AIR AT 1560 F (45)

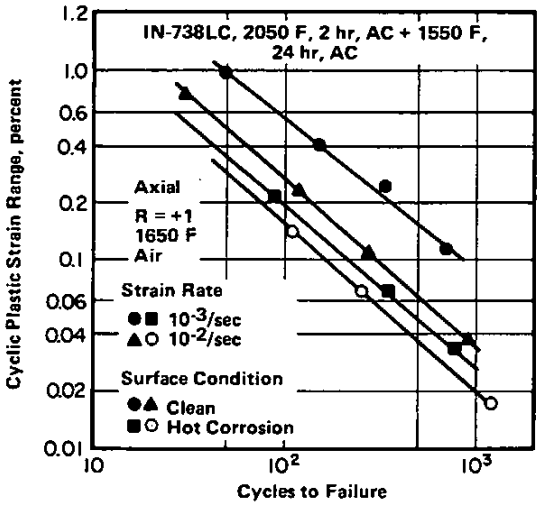

FIGURE 3.056. EFFECTS OF STRAIN RATE AND HOT-CORROSIVE CONDITIONS ON FATIGUE LIFE AS A FUNCTION OF CYCLIC PLASTIC STRAIN RANGE AT 1650 F (41)

Hot-corrosion conditions induced by coating specimens with a mixture of 75 percent sodium sulfate and 25 percent sodium chloride.

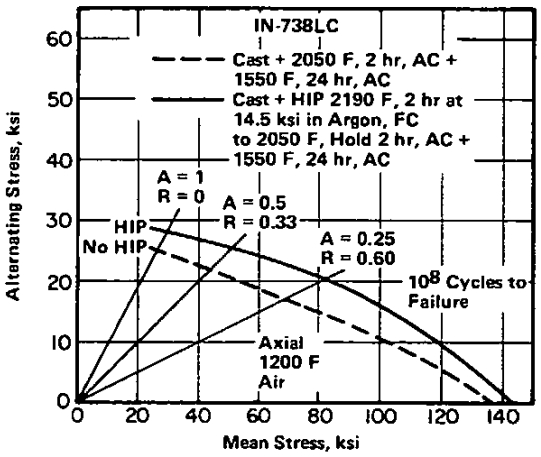

FIGURE 3.057. STRESS-RANGE DIAGRAM FOR THE LOW-CARBON VERSION, IN-738LC, SHOWING THE EFFECT OF HOT ISOSTATIC PRESSING (HIP) ON COMBINATION OF MEAN AND ALTERNATING STRESSES REQUIRED TO CAUSE FATIGUE FAILURE IN 10^8 CYCLES AT 1200 F (32)

	Ni
16	Cr
8.5	Co
3.5	Al
3.5	Ti
2.6	W
1.8	Mo
0.9	Cb

IN-738

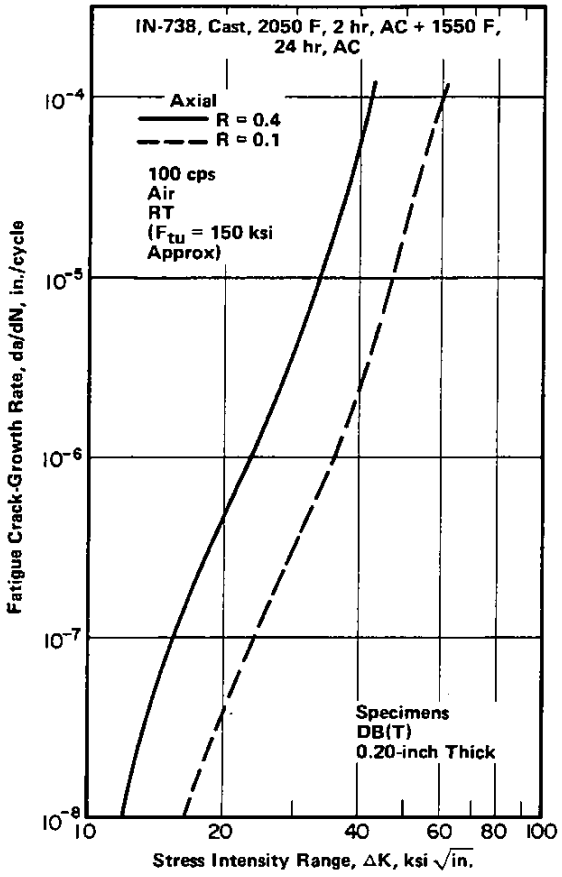

FIGURE 3.058. EFFECTS OF VARIATIONS IN STRESS INTENSITY RANGE AND STRESS RATIO ON FATIGUE CRACK-GROWTH RATE AT ROOM TEMPERATURE (9)

For explanation of specimen type see Reference 42. Orientation designations do not apply to castings.

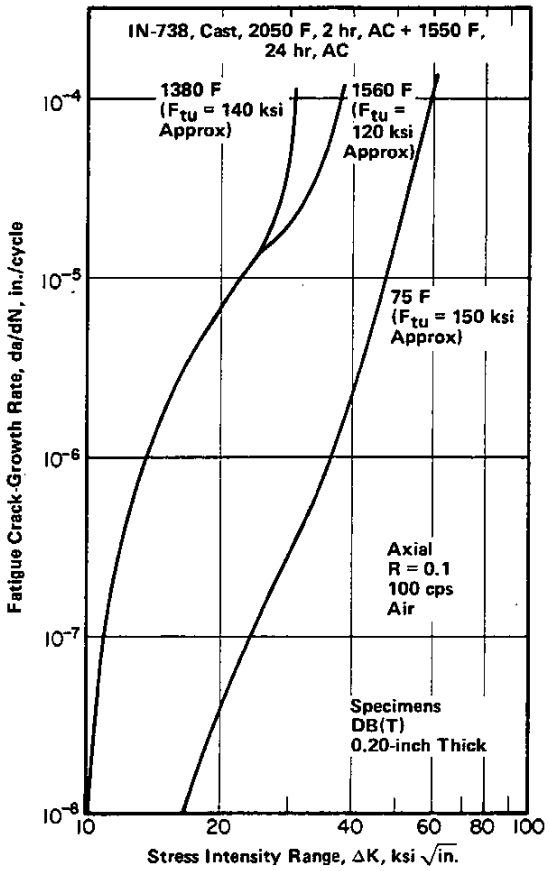

FIGURE 3.059. EFFECTS OF VARIATIONS IN STRESS INTENSITY RANGE AND TEMPERATURE ON FATIGUE CRACK-GROWTH RATE (9)

	Ni
16	Cr
8.5	Co
3.5	Al
3.5	Ti
2.6	W
1.8	Mo
0.9	Cb

IN-738

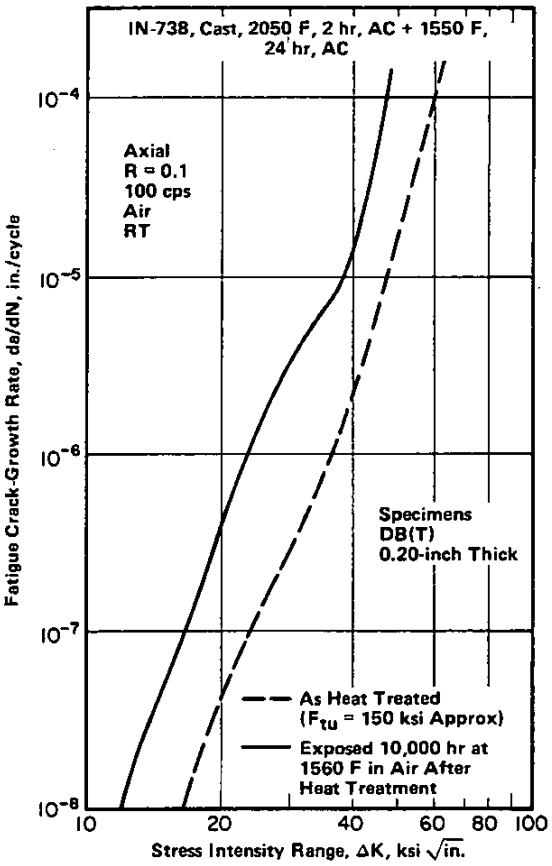

FIGURE 3.0510. EFFECTS OF VARIATIONS IN STRESS INTENSITY RANGE AND OF LONG-TIME EXPOSURE AT 1560 F IN AIR ON FATIGUE CRACK-GROWTH RATE AT ROOM TEMPERATURE (10)

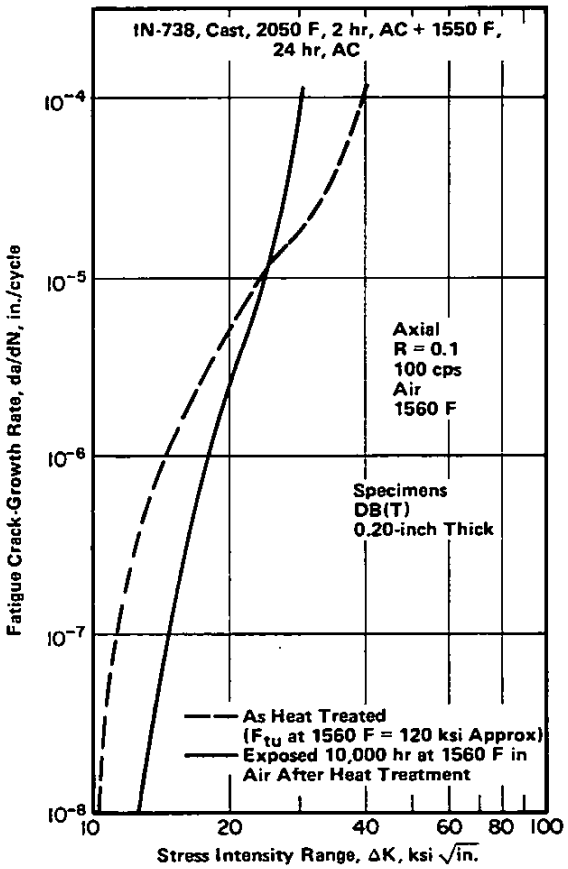

FIGURE 3.0511. EFFECTS OF VARIATIONS IN STRESS INTENSITY RANGE AND OF LONG-TIME EXPOSURE AT 1560 F IN AIR ON FATIGUE CRACK-GROWTH RATE AT 1560 F (10)

Ni
16 Cr
8.5 Co
3.5 Al
3.5 Ti
2.6 W
1.8 Mo
0.9 Cb

IN-738

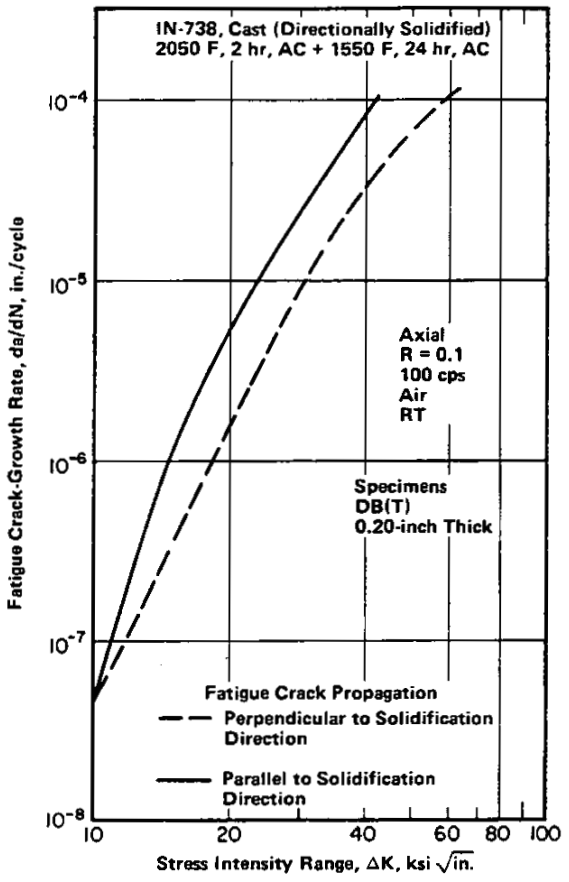

FIGURE 3.0512. EFFECTS OF VARIATIONS IN STRESS INTENSITY RANGE AND ORIENTATION ON FATIGUE CRACK-GROWTH RATE AT ROOM TEMPERATURE IN DIRECTIONALLY SOLIDIFIED CASTINGS (11)

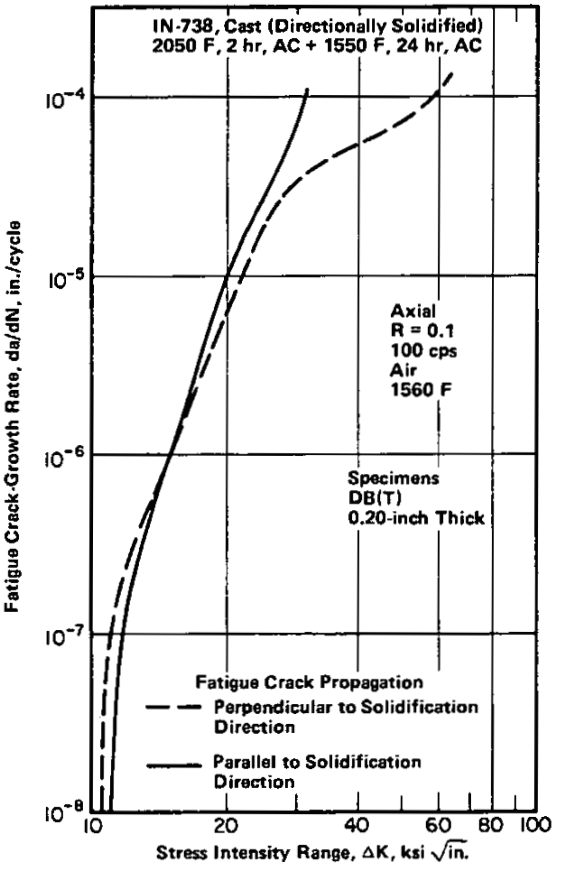

FIGURE 3.0513. EFFECTS OF VARIATIONS IN STRESS INTENSITY RANGE AND ORIENTATION ON FATIGUE CRACK-GROWTH RATE AT 1560 F IN DIRECTIONALLY SOLIDIFIED CASTINGS (11)

Ni
16 Cr
8.5 Co
3.5 Al
3.5 Ti
2.6 W
1.8 Mo
0.9 Cb

IN-738

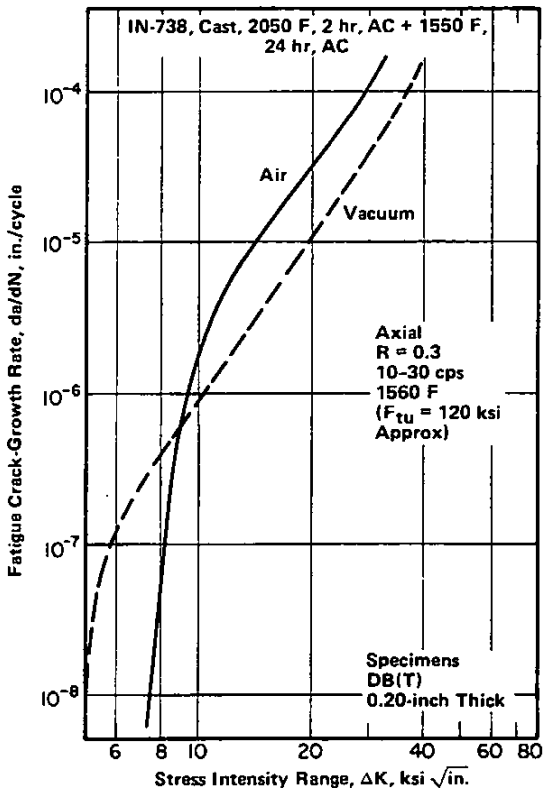

FIGURE 3.0514. FATIGUE CRACK-GROWTH RATE AS A FUNCTION OF STRESS INTENSITY RANGE IN AIR AND VACUUM AT 1560 F (36)

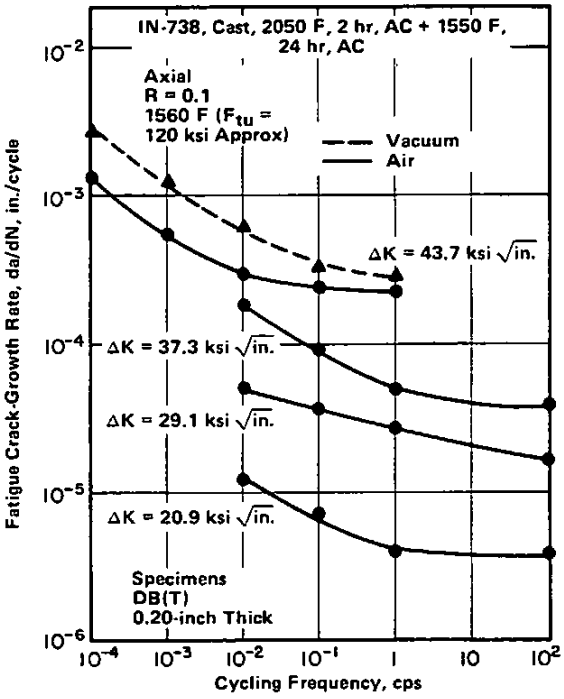

FIGURE 3.0515. EFFECT OF CYCLING FREQUENCY AND STRESS INTENSITY RANGE ON FATIGUE CRACK-GROWTH RATE IN AIR AND VACUUM (30)

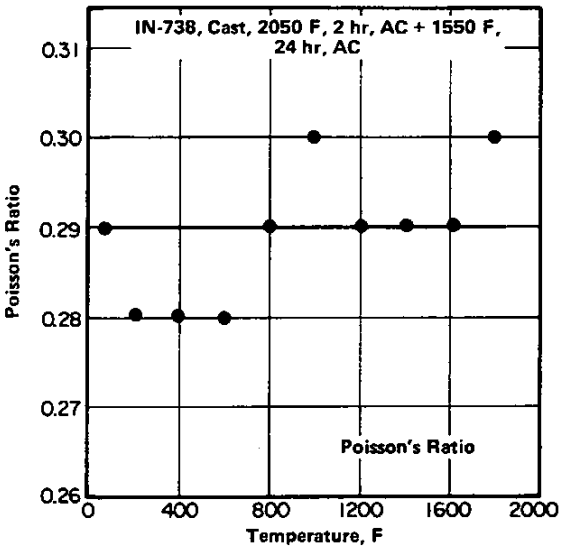

FIGURE 3.0611. POISSON'S RATIO AT TEMPERATURES FROM 75 F TO 1800 F (2)

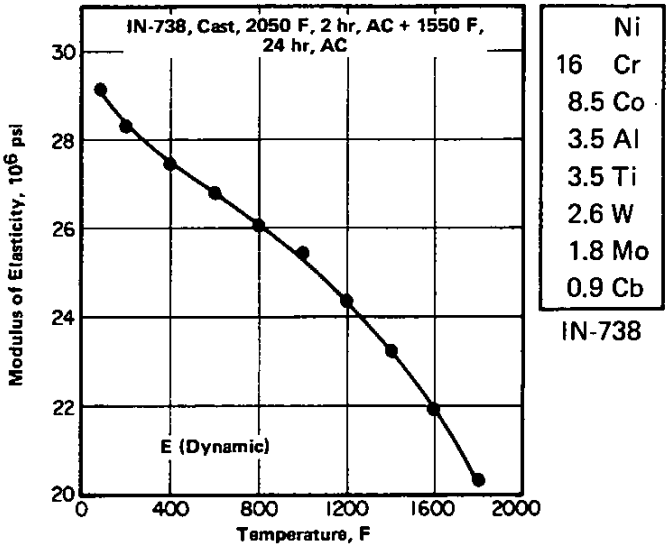

FIGURE 3.0621. EFFECT OF ELEVATED TEMPERATURES ON MODULUS OF ELASTICITY (2)

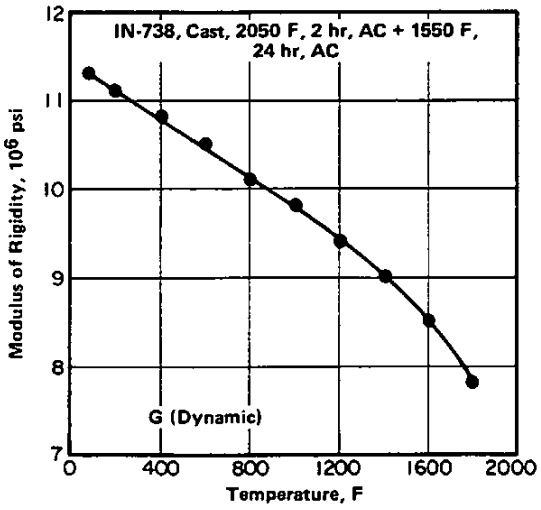

FIGURE 3.0631. EFFECT OF ELEVATED TEMPERATURES ON MODULUS OF RIGIDITY (2)